Exploring the impact of soil compaction on relative transpiration by potatoes

A case study performed at 'Van Den Borne Aardappelen'

MSc Thesis by Nico-Jan Bakker

15 July 2014

WAGENINGEN UNIVERSITY
WAGENINGEN UR

Exploring the impact of soil compaction on relative transpiration by potatoes, A case study performed at ‘Van Den Borne Aardappelen’

Study program

MEE – MSc Earth and Environment

Specialisation Soil Geography and Landscape

Student registration number

881225030010

Thesis code

SGL – 80436 / 36 ECTS

Supervisors

Jetse Stoorvogel (Wageningen University)

Jos Van Dam (Wageningen University)

Lammert Kooistra (Wageningen University)

Date

15 July 2014

Wageningen University, Wageningen

Abstract

Soil compaction is recognised as a serious threat for agriculture but there is lack of data about the actual extent of soil compaction that can be used to validate this risk assessments. Differences in crop development and soil moisture might be useful indicators for the detection of soil compaction. Both indicators are linked to relative transpiration. This research investigates the relation between relative transpiration and soil compaction in order to see whether relative transpiration can be used as indicator for soil compaction. Soil compaction, soil hydraulic characteristics and other soil characteristics that influence soil hydraulic characteristics were measured at 23 locations within a field located in the Southern part of the Netherlands. The derived soil hydraulic characteristics were used to model relative transpiration. Differences in modelled relative transpiration and soil hydraulic characteristics between different locations were compared with differences in soil compaction and other soil characteristics in order to investigate to what extent differences in relative transpiration could be explained by differences in the degree of soil compaction. Highest values for relative transpiration were calculated at locations with relatively strong signs of soil compaction, a deep A horizon and high organic matter contents. For locations were one of this characteristics was not present calculated values for relative transpiration were lower. The influence of soil compaction and organic matter content were also visible in measured hydraulic characteristics. For locations where both the degree of soil compaction and organic matter content were high also highest values for water retention capacity and hydraulic conductivity were found.

Acknowledgements

First of all I would like to thank Jacob van den Borne for allowing me to do this research on his field. Thanks for allowing me to dig 23 profile pits in the field and doing different measurements on his ground. I appreciated very much that he borrowed me a small excavator which saved me a lot of work.

This also I would also like to thank my supervisors Dr. Jetse Stoorvogel, Dr. Jos van Dam and Dr. Lammert Kooistra for supporting me in the different phases of my MSc thesis. I would like to thank Jetse Stoorvogel for the time he spent with me in the field. He supported me with questions around practial issues and gave me a hand to explore the study site. I would like to thank Jos van Dam for is help with the analyses of the lab experiments as well as his information on the SWAP model. Furthermore, I thank Lammert Kooistra for bringing me into contact with Jacob van den Borne. Without him, this whole project would not have been possible.

For practical support during the labwork my thank goes to Hennie Gertsen.

Furthermore I would also like to thank friends and family that supported me during my master and especially during the time I worked on my thesis. Thanks for being there when I needed you!

Table of Contents

1. Introduction

1.1 Soil compaction

Soil compaction is described as the process in which a certain soil mass is forced to occupy a smaller volume than previously *(Young, 2012)*. The compaction is caused in two directions, namely by vertical stresses related to gravity and horizontal stresses related to slipping wheels and tillage activities *(Batey, 2009)*. This means in practice, that soils can be compacted by tractors and other agricultural equipment and by the hooves of grazing livestock and other animals *(Batey, 2009)*.

Soil compaction can become a serious problem as it alters fundamental physical soil characteristics, like for example a denser arrangement of soil particles, a decrease in porosity, an increase in the dry bulk density and an increase in penetration resistance by roots *(Young, 2012; Reintam et al., 2009; Batey & McKenzie, 2006)*. These physical changes influence both the air content of the soils as well as the distribution of water. A decrease in porosity and an increase in the dry bulk density will immediately lead to changes in the hydrological properties of the soil, affecting both the water retention curve as well as the hydraulic conductivity function of the soil *(Wösten et al., 1995)*. Altered soil hydraulic characteristics, on their turn, may influence soil chemical and biological processes that are important for the nutrient supply of plants *(Batey & McKenzie, 2006; Reintam et al., 2009)*.

In the past decades different technical solutions were proposed by machinery manufacturers that increase the contact surface to spread the pressure of agricultural equipment on the soil *(Vermeulen, 2013)*. However, they only partly succeeded as at the same time, the weight and size of agricultural equipment increased. Due to greater contact areas of equipment with the ground, the higher forces penetrate deeper into the soil *(Håkansson and Reeder, 1994)*. Therefore, the increase of pressure on the subsoil is higher compared to the pressure on the topsoil *(Vermeulen, 2013)*. This is a serious threat for agriculture because the subsoil has a lower resilience to compaction, and, once it is there, the compaction is more persistent compared to compaction of the topsoil *(Van den Akker & Hoogland, 2011)*. This differences can be explained by a decrease of intensity and frequency of factors that alleviate soil compaction, e.g. intensity and frequency of biological activity, tillage, wetting/drying and freezing/ drying processes decrease with depth *(Håkansson and Reeder, 1994)*.

For the Netherlands it is estimated that 50% of the clay soils and, depending on the region, between 10% and 45% percent of the Sandy soils has an over compacted subsoil *(Van den Akker & Hoogland, 2011)*. In western and eastern Europe, 11% of the total land area is affected by soil compaction, and thus making it a serious threat for plant growth *(Van den Akker et al., 2003)*. The European Union recognises soil compaction as one of the most severe threat for European soils *(CEG, 2006; Vermeulen, 2013)*. Priority areas are assigned, were subsoil compaction is expected to take place, to prevent further compaction of the subsoil in these areas *(Edelenbosch, 2011)*. Accurate data about the actual extend of subsoil compaction in the Netherlands is hardly available *(Van den Akker & Hoogland, 2011; Edelenbosch, 2011)*. Up until now, subsoil compaction risk assessments are used to determine affected areas but results are questionable as there is a lack of good data to validate these assessments *(Van den Akker & Hoogland, 2011; Edelenbosch, 2011)*. Therefore, more effort is needed to improve the validation strategy, which can be achieved by gathering more data about the extension of soil compaction nationwide. A possible way to do so is to extend the Dutch national soil data base by adding information about soil compaction *(Edelenbosch, 2011)*.

1.2 Detection of soil compaction

Use of modern sensing techniques, both proximal and remote, are proposed as a possible way to gather information about soil compaction and then extend the national soil database *(Edelenbosch, 2011)*. Zwart et al. (2011) proposed the use of remote sensing data about soil moisture as useful indicators for soil compaction, but that further study towards their usability, as an indicator for subsoil compaction, is still needed. Furthermore, information on crop development could serve as an indicator for soil compaction *(Reintam et al., 2009)*.

Microwave remote sensing can be used to observe soil moisture contents of the soil surface or, if present, vegetation cover *(Scott et al., 2003)*. The named study also presents a method, called SEBAL, which allow determining latent heat flux. The latent heat flux can subsequently be compared with potential evapotranspiration data to derive an indirect measure for the water deficit in the root zone *(Scott et al., 2003).* The following step would be to get a better understanding of the relation between water deficits and soil compaction. The results of a study that investigates this relationship can give indication whether soil moisture is suitable for the detection of soil compaction, as proposed by Zwart et al. (2011).

In general, modern sensing techniques are already used to map spatial variation in crop development at a field scale, in order to support precision farming *(Kooistra, 2011)*. Additionally, the information gathered on crop development may also serve as an indicator for soil compaction. Different studies present soil compaction as the causation of significant yield losses and negative impacts on plant growth, meaning that crop development is limited *(Reintam et al., 2009; Van den Akker et al., 2003)*. However heterogeneity of crop development within a field can be due to soil compaction but also due to other factors. The relative role of subsoil compaction compared to other factors is not yet well understood *(Wilcox et al., 2000; Van den Akker & Groot, 2007; Lamberink, 2013)*.

Soil moisture and crop development, which can as previously stated serve as an indicator for soil compaction, are both linked to transpiration *(Ehlers and Goss, 2003)*. Transpiration is characterized by actual and potential transpiration and describes the evaporation of water by vegetation. Potential evaporation was firstly characterized by weather conditions (energy available and turbulence present) and the assumption that enough moisture is available in the ground *(Penman, 1948)*. It has been extended by vegetation specific parameters and can thus be used to determine potential transpiration *(Montheith, 1965)*. Actual transpiration however depends on the availability of moisture present in the root zone of the plant *(Ehlers and Goss, 2003)*.

Potential transpiration can relatively easy be calculated by using meteorological data, which is usually widely available *(Tanner and Pelton, 1960)*. The ratio of actual to potential transpiration indicates drought stress for plants and is directly linked to crop yield *(Ehlers and Goss, 2003)*. Up until now, no literature is available that indicates whether transpiration can server as a measure for soil compaction. This study will identify whether a relation between transpiration and soil compaction can be found for a field in the Netherlands.

1.3 Research objective and questions

The aim of this study is to propose indicators that characterize soil compaction. For this the relationship between hydrological characteristics and soil compaction within a field in the South of the Netherlands is identified. The results are furthermore linked to other soil characteristics. The derived results allow giving suggestions on relevant indicators that can be used to assess soil compaction.

The main research question of this study is the following:

How can soil characteristics together with transpiration data characterize soil compaction?

This research question is linked to the following sub-questions:

- To what extent does soil compaction takes place within the A horizon of a particular field in the south of the Netherlands?
- How do organic matter content, the depth of the A horizon and electronic conductivity vary within the investigated field?
- How are soil hydraulic properties of the A horizon related to soil compaction and organic matter content and electronic conductivity?
- How is transpiration, modelled from field measurements and observed meteorological data, connected to soil characteristics?

The answer of the research question is derived by gathering field data and a model study. First, a field in the south of the Netherlands is chosen and 23 locations in this field chosen. For all locations soil compaction is quantified by determination of dry bulk density, penetration resistance and visual observation. Additionally, the depth of the A-horizon, the organic matter content in this and the level of ground water is determined and the water retention measured. The gathered data serves together with meteorological data from a nearby weather station as input for the SWAP model. The model allows estimating the ratio between actual and potential transpiration. The ratio of actual to potential transpiration is for each location correlated to compaction of soil and the depth of the A horizon as well as the organic matter content.

First the chosen research location is described. Followed by a description of the different methods used to determine soil compaction, and the other soil characteristics relevant for describing spatial variability of the soils within the field. This soil characteristics include elevation differences, electronic conductivity, organic matter content, the depth of the A horizon and soil hydraulic properties. After this the procedure followed for the modelling part is described. Within the results and discussion section first the measured soil characteristics are discussed. Followed by the results of the Evaporation modelling. The last Chapter of this work is used to answer weather different soil characteristics together with transpiration data can be used to characterize soil compaction, and if needed recommend further research.

2. Materials and methods

2.1 Research location and climate

2.1.1 Van den Borne Aardappelen

The research was conducted at Van den Borne Aardappelen, an arable farm in southern part of the Netherlands near the village of Reusel. Both the farmer and Wageningen University are already cooperating in the 'making sense' project. Main goal of this project is to develop a decision module for the management of soil fertility and fertilization of agricultural crop that is based on different sources of information and different calculation modules (Borne, 2013). At the farm a lot of data about plant growth and soil fertility is collected with different techniques, both by the different partners of the making sense project as well as by the farmer himself. In consultancy with the farmer a particular field was selected to perform this research. Decision for a particular field was based on possible presence of human induced soil compaction and to the utility of doing research at that particular field for the farmer and the making sense project.

Figure 1 Research location, located near Reusel at the border between Belgium and the Netherlands.

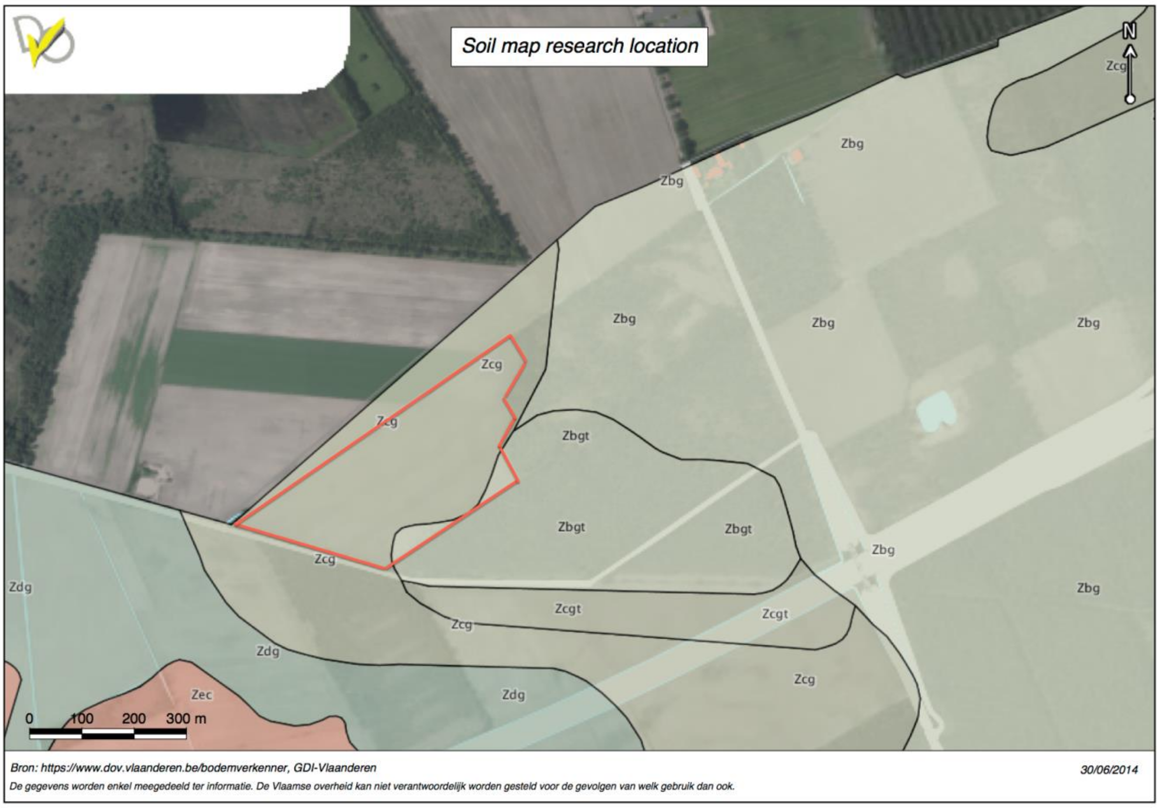

Figure 2 Research location displayed on a soil map, derived from Databank Ondergrond Vlaanderen *(GDI-Vlaanderen, 2014)*. The research location is located in Belgium just outside the Netherlands and indicated through the red lines. Soil types are: Zec = wet sandy soils with interrupted B horizon , Zbg = moderately wet sandy soils with a clear B horizon , Zcg = moderately dry sandy soils with a clear B horizon, Zdg = dry sandy soils with a clear B horizon.

2.1.2 Field characteristics

The research was conducted at an arable field with a size of 10.55 Hectare at 700m distance from the farm. The field is located in Belgium at 51˚31'10'' Northern Latitude and 5˚16'80" Eastern Longitude. At the east and the south the field is bordered by pine forest and to the north and west by arable fields. In general land use in the surrounding areas is characterized by arable fields and pine forest.

The soil of the field was classified as a dry sandy soil with a clear B-horizon (Figure 2). During a first exploration of the soil profile a black sandy A horizon, +/- 50cm deep, was distinguished from a white colored sandy C horizon. Podzol B-horizons were not found during the first exploration, although its presence was suggested by the results of a more detailed profile examination. Results of this more detailed profile descriptions will be described in section 3.2.2. . The white sandy C horizon showed measurement a high penetration resistance (>3MPa) during a first explorative measurements, which indicates the presence of a compacted layer.

2.1.3 Climatological characteristics

Climatological characteristics were derived from weather station Eindhoven, located 21km north east of the research field, at 51˚31' Northern Latitude and 5˚23' Eastern Longitude. The field is located in an area with a maritime temperate climate. Daytime temperatures vary between 5.4 C in January and 22.8 C in July while average night time temperature ranges from -0.2 C to 12.3 C (Figure 3). Monthly precipitation amounts are, on average, constant throughout the year, varying between 44mm and 77mm per month (Figure 4). During the months April until August the potential evaporation usually exceeds the amount of precipitation, which results in accumulating precipitation deficits in these time of the year.

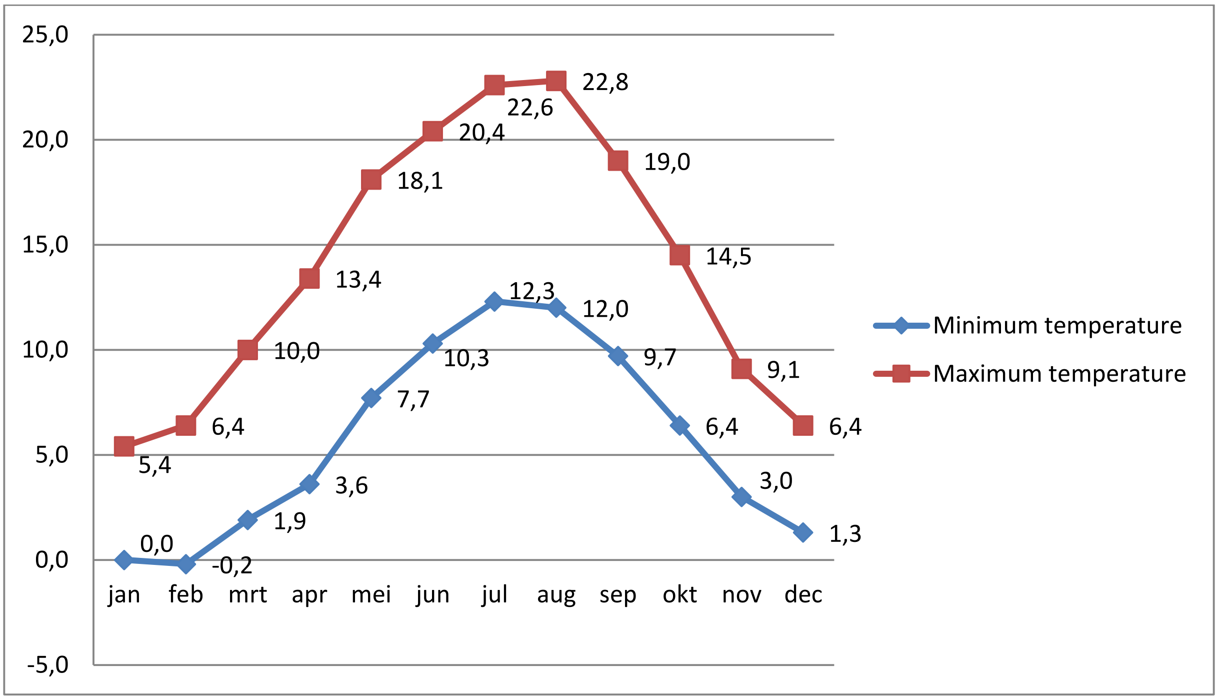

Figure 3 Average monthly minimum and maximum temperatures between 1985 and 2011 at KNMI station Eindhoven. Source: KNMI

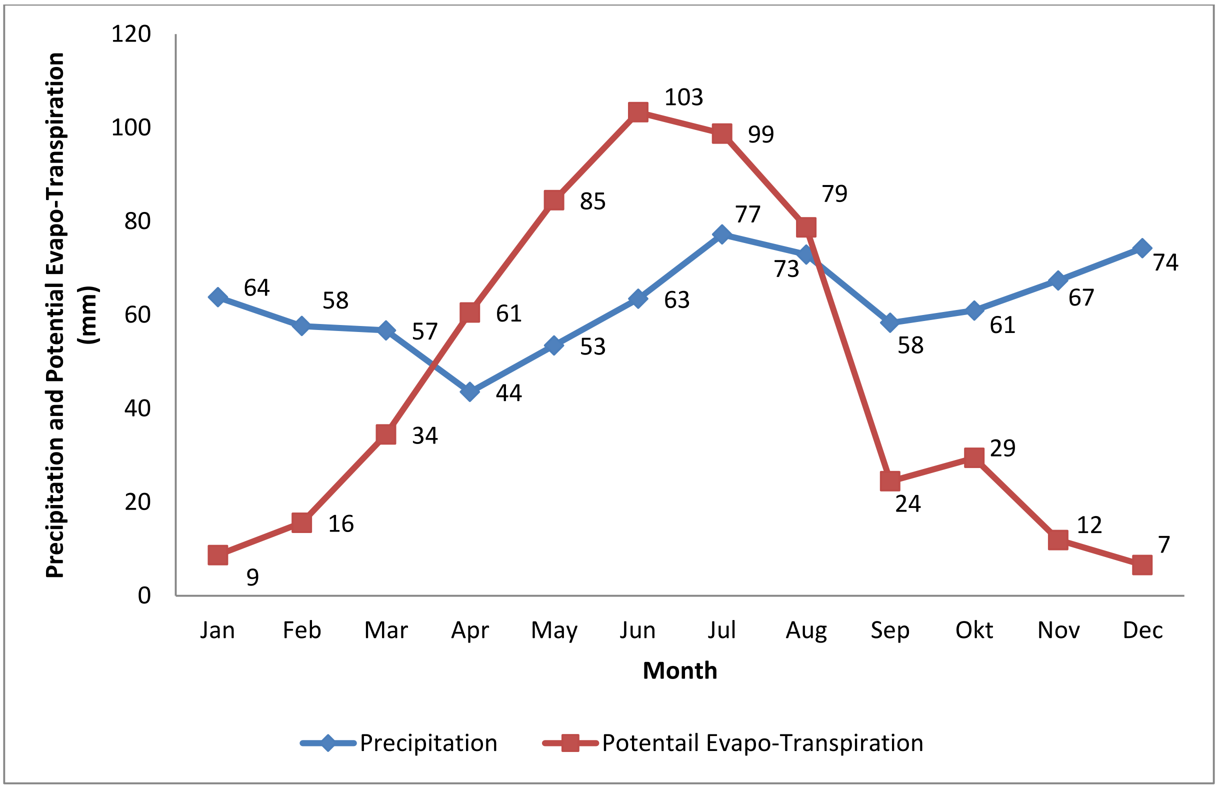

Figure 4 Average monthly precipitation and potential Evapo-Transpiration between 1985 and 2011 at KNMI station Eindhoven. Source: KNMI.

2.1.4 Field management

For at least the past 5 years the field was used as arable land, with either potatoes or sugar beets growing. Only the topsoil was disturbed by annual tillage practice while the subsoil remained largely untouched. Irrigation is applied when potatoes are grown. Previous year the field was cultivated with sugar beets. This year potatoes are grown.

2.2 Determination of soil compaction

Different techniques were used to determine soil compaction. Figure 5 shows a sketch of the field and the selected sampling points for all measurements. Sampling was conducted at the locations that are indicated through red points (23 in total). They are located in two rows with a distance of 80m in between each other, along two transects parallel to the longest side of the field. Orientation of the transects in this direction was done for two reasons. First because it enabled to capture most of the differences in elevation differences within the field, which are described in section 3.2.1, second because in this direction tracks formed by the GPS navigated machinery of the farmer could be used for allocation of the transects. The exact amount of measurement location and their distance in between was based on the available amount of time of this research.

The following paragraphs will explain the different techniques applied to quantify soil compaction in this study, namely visual soil-profile examination, penetration resistance and dry bulk density.

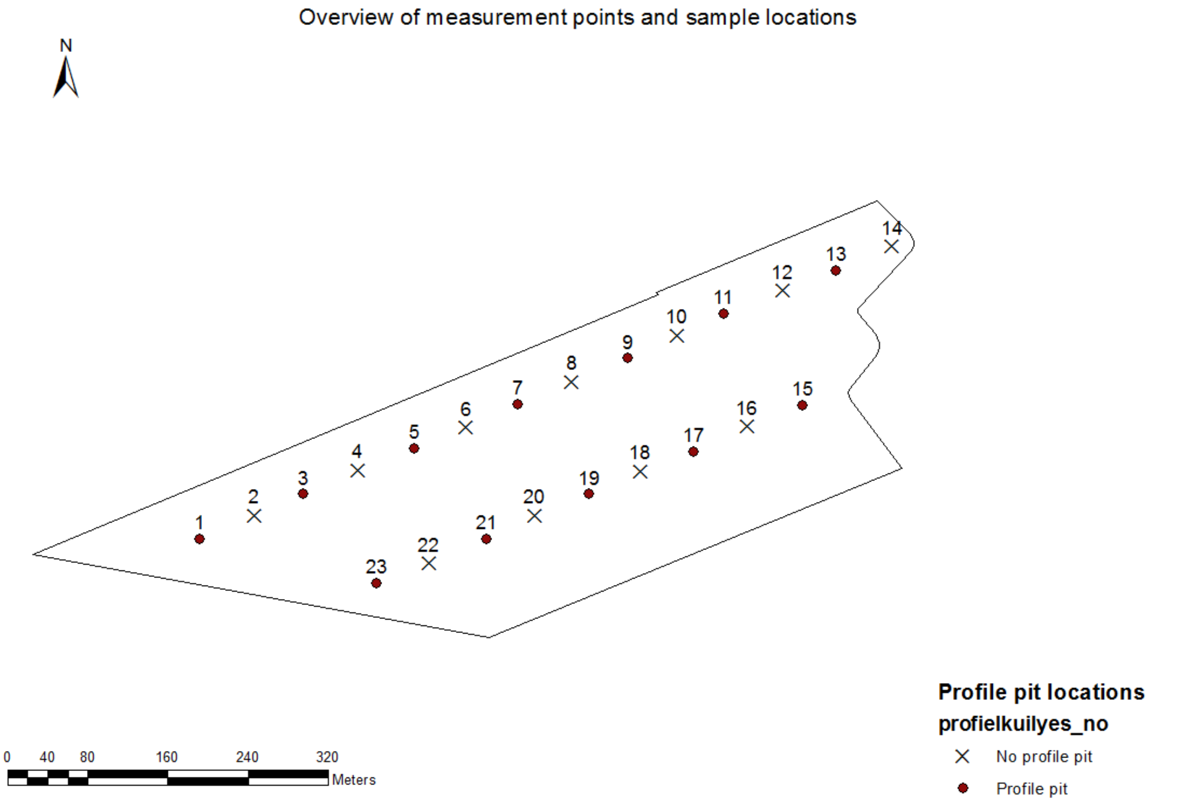

Figure 5, Overview of sample locations. Explorative measurements were conducted at every location, more detailed soil measurements and soil profile descriptions were conducted only at location indicated with a red dot.

2.2.1 Visual soil-profile examination

The soil profile description was conducted in order to: i- identify possible compacted soil layers and the depth at which they occur, ii- to describe and sample the different soil layers as input for further analyses and modelling in SWAP and iii- to observe possible unexpected geomorphological characteristics that were not expressed by the soil map. Because human induced soil compaction often appears in the plough pan, between 20 and 50cm depth profile pits were digged to a minimum depth of 60cm *(Vermeulen, 2013; Van den Akker & De Groot, 2007)*

Changes in physical properties because of soil compaction can be assessed by a careful visual examination of the vertical face of the profile pit *(Batey & McKenzie, 2006)*. This can be done by removing loose soil from the face of the profile pit to expose the more compact soil layer, which is more difficult to remove *(Batey & McKenzie, 2006)*. In this way more compacted layer can become visible. During the visual soil profile examination, the different horizons were identified and their depth measured.

2.2.2 Penetration resistance

Penetration resistance, as a function of depth, was used to get determine the degree of soil compaction and the depth at which it occurs. Penetration resistance was measured with a manually operated penetrometer at the same locations as pits were made. Penetrometer measurements can be a valuable measurement to determine soil compaction. Together with profile pit examination these measurements can help to determine the reason for differences in penetration resistance *(Spoor et al., 2003)*. Threshold values for soil compaction were derived from literature and based on the maximum penetration resistance at which roots can still penetrate the soil. Below 1.5 MPa no problems with rooting are expect, above 3 MPa rootability was indicated as bad *(Locher, 1987)*. To differentiate the degree of soil compaction, threshold values of 1.5, 2 and 2.5 MPa were used. Depths at which threshold values were exceeded were compared with depths of the different natural horizons to see whether compaction was part of a natural compacted layerorinduced by human influence.

2.2.3 Dry bulk density

Undisturbed ring samples were taken vertically from the top part of the horizon. For the A horizon and possible compacted A horizons this was done at least one time for every location For the C horizon this was only done for location 3 and 21 and for the Ap horizon for location 7, 9 and 10.

Dry bulk densities were measured to quantify the degree of compactness of a certain soil layer. Especially for sandy soils, the soil bulk density is a good indicator for the degree of compactness of a soil *(Van den Akker & De Groot, 2007)*. Dry bulk density was determined following the core method *(Blake, 1986)*. For this method undisturbed soil samples were collected in sample rings with a known volume. After being used for the determination of the water retention curves the samples were dried at 105 degree Celsius for 24 hours.

The dry bulk density was derived according to the following formula:

$$\rho_d = \frac{M_s}{V_s} = \frac{M_c - M_r - M_l}{V_s}$$

With:

ρ_d = *Dry bulk density of the soil (g/cm3)*

M_s = *Mass of the oven-dried soil (g)*

V_s = *Volume of sample ring (cm3)*

M_c = *Mass of the oven-dried soil core including lid and ring (g)*

M_r = *Mass of the sample ring (g)*

M_l = *Mass of the lid (g)*

2.3 Determination of other soil parameters that influence hydraulic properties

Spatial within field variability was also determined for other soil parameters that might influence soil hydraulic properties of the soil. From literature it was derived that hydraulic properties of sandy soils are mainly influenced by organic matter contents, dry bulk density, average grain size of sand particles and the clay and silt percentage *(Wösten, 1997)*.

Soil organic matter contents, average grain size of sand particles and clay and silt percentage were measured at the previously named locations. For every measuring point, the electronic conductivity was additionally determined, since its results help to classify soil texture. From the gained data, spatial within field variation of soil compaction was determined with different methods, which are described in the following paragraphs.

2.3.1 Electronic conductivity

Electronic conductivity of a soil was measured with an EM-38 scanning device at the 23 named locations. According to literature EM-38 scans can be used to map spatial variability of different soil properties such as soil salinity, soil texture & texture changes and water content *(Hoefer et al., 2010; Wong et al., 2010).* It also has the potential to indicate spatial patterns in soil compaction *(Hoefer et al., 2010; Wong et al., 2010)* The EM-38 sensor measures electronic conductivity of the field at 0-40 cm depth and at 0-90cm depth. Depth ranges are 10cm smaller compared to official depth ranges mentioned by the manufacturer of the sensor because the sensor was placed on a 10cm high sled in order to be able to easily pull it over the field. The Electronic conductivity scan was conducted in perpendicular rows with 4.5 m distance in between. Results of the scan were interpolated using ordinary kriging and used to get insight in the spatial within field variability of the different soil characteristics in this field.

Formulas for the zero-measurement calibration of measured EC values were derived from the operating manual of the EM-38 device *(GEONOMICS LIMITED, 2008)*. Formula for the temperature calibration was derived from Ruijun et al. (2007).

$$EC_s = (QP_{raw} - QP_C) * f_T$$

$$QP_C = 2 * QP_V - 2 * QP_H$$

With:

EC_s = *Electronic conductivity of the soil (mS/m)*

QP_{raw} = *Electronic conductivity measured by the EM-38 sensor (mS/m)*

QP_C = *Calibrated zero value of the electronic conductivity (mS/m)*

QP_V = *Electronic conductivity during calibration in Vertical position (mS/m)*

QP_H = *Electronic conductivity during calibration in Horizontal position (mS/m)*

$$f_T = 0{,}447 + 1.4034 * e^{\left(-T/_{26.8151}\right)}$$

T = *Measured temperature (C)*

In order to derive spatial electronic conductivity data, the measurements were interpolated using Ordinary Kriging. Kriging is used because it is assumed to be the best linear unbiased predictor *(Cressie, 1990)*. Altitude values were also measured with EM-38 scan. This data was also kriged for the same reason. The interpolated data was spatially averaged to present it as isolines..

2.3.2 Organic matter content

Organic matter content was measured to characterize different soil layers and for the determination of soil hydraulic properties with pedotransfer functions. For determination of the organic matter content the A and Ap horizon were sampled as one layer. This was done for every location. The C horizon, however, was only sampled at location 1 to 9 and location 21 and 23. The organic matter contents were averaged for the C horizon. The Organic matter content was derived with the loss of ignition method. *(Howard, 1965)* For this purpose oven dried soil samples (24 hours at 105 °C) were ignited 3 hours at 550 °C (Howard & Howard, 1990; Howard, 1965). The organic matter content was calculated by dividing the total mass loss during the ignition by the weight of the oven dried soil before ignition as shown in the following formula.

$$OM = \frac{M_{105} - M_{550}}{M_{105} - M_{cup}} * 100\%$$

With:

OM = Organic matter content (%)

M_{105} = Mass of cup with oven dried soil (g)

M_{550} = Mass of cup with soil after ignition (g)

M_{cup} = Mass of empty cup (g)

2.3.3 Soil texture

M50 median sand grain size and Clay Silt percentage will be determined from the profile pits. They can later serve as input for pedotransfer functions *(Wösten et al., 1995)*. Median sand grain size were determined by using a sand ruler. Clay and Silt percentages were determined by sieving method, using a 50µm sieve *(Klute, 1986)*. The sieving was done for two randomly selected soil samples (location 1 and location 7) from the combined A/Ap horizon to determine average clay silt percentage of this horizon. The total percentage of clay and silt of the C horizon was based on only one sample (location 7).

2.4 Determination of soil hydraulic properties

2.4.1 Water retention measurements

Water retention curves were determined in the lab using the sandbox apparatus method for low suctions (>-200 cm) and pressure membrane method for higher suctions (< -1000cm) *(Klute, 1986)*.

For the sandbox apparatus method undisturbed soil samples with a known volume were collected. For every profile pit at least one sample of the A horizon was taken, while samples of the Ap and C horizon were only taken at a few locations. An overview of collected ring samples is given in Table 1.

Mass of the ring samples was measured at saturation and at pF1, pF1.5 and pF2. Weight differences with oven dried samples was used to determine volumetric water contents at different suctions as seen in the formula below.

$$\theta = \frac{V_w}{V_s} = (M - M_d)/V_s$$

With:

θ = Volumetric soil moisture content (-)

V_w = Volume of soil moisture (cm3)

V_s = Volume of sample (cm3)

M = Mass of soil sample at specific soil water pressure head (g)

M_d = Mass of oven dried soil sample (g)

V_s = Volume of sample ring (cm3)

For the pressure membrane method bulk sample of loose soil material were used. For every location one composite sample of the Ap and A horizon was taken, except for location 11 were they were sampled separately. The C horizon was only sampled at 4 locations (Table 2). For every sample the weight was measured at pF 3 and pF 4.2. The following formulas were used to convert measured weights into volumetric soil moisture contents.

$$\omega = \frac{M_w}{M_d} = (M - M_d)/M_d$$

$$\theta = \rho_d * \omega$$

With:

ω = Gravimetric moisture content (-)

M_w = Mass of soil moisture (g)

M_d = Mass of oven dried soil sample (g)

M = Mass of soil sample at specific soil water pressure head(g)

θ = Volumetric soil moisture content (-)

ρ_d = Dry bulk density of the soil (g/cm3)

2.4.2 Fitting water retention curves

The soil water retention function is described by the formula below *(Genuchten, 1980)*

$$\theta(h) = \theta_{res} + \frac{\theta_{sat} - \theta_{res}}{(1 + |\alpha h|^n)^{\frac{n-1}{n}}}$$

With:

$\theta(h)$ = Volumetric moisture content as function of soil water pressure head (-)

θ_{res} = Residual moisture content (-)

θ_{sat} = Saturated moisture content (-)

α = Shape parameter (cm-1)

n = Shape parameter (-)

h = Soil water pressure head (cm)

The described water retention function was fitted to the measured soil moisture contents by manually curve fitting in Excel. For the A horizon this was done for every location separately while for the Ap and C horizon the retention function was fitted to the average of all locations. Average moisture content of the Ap horizon was determined by averaging over locations 7, 9 and 11 while average for the C horizon was take from location 3 and 21. Fitted water retention curves were used in SWAP to model soil- water flow and plant growth at different locations.

2.4.3 Determination of hydraulic conductivity function

The hydraulic conductivity function is described by *(Mualem, 1976)*

$$K(h) = K_{sat} \frac{\left[(1+|\alpha h|^n)^{1-1/n} - |\alpha h|^{n-1}\right]^2}{(1+|\alpha h|^n)^{(1-1/n)(\lambda+2)}}$$

With:

K(h) = Hydraulic conductivity as function of soil water pressure head (cm/d)

K_{sat} = Saturated hydraulic conductivity (cm/d)

λ = Shape parameter (-)

The hydraulic conductivity function was not determined with lab experiments only but with use of pedotransfer functions as well. Used pedotransfer functions are determined for cover sands in the northern part of the Netherlands. For this research it was assumed that they are also suitable for cover sands in the south *(Wösten et al., 1995)*.

$$\mathrm{K_s} = 9{,}5 - 1{,}471 * \rho\mathrm{d}^2 - 0.688 * \mathrm{OM} + 0{,}0369 * \mathrm{OM}^2 - 0{,}332\ln(\mathrm{CS})$$

$$\alpha = 146{,}9 - 0{,}0832 * OM - 0{,}395 * topsoil - 102{,}1 * \rho\mathrm{d} + 22{,}61 * \rho\mathrm{d}^2 - 70{,}6\rho\mathrm{d}^{-1} - 1{,}872 * CS^{-1} - 0{,}3931 * ln(CS)$$

$$\mathrm{n} = 1092 + 0{,}0957 * \mathrm{CS} + 1.336 * \mathrm{M50} - 13{,}229 * \mathrm{M50}^{-1} - 0{,}001203 * \mathrm{M50}^2 - 234{,}6 * \ln(\mathrm{M50}) - 2{,}67 * \rho\mathrm{d}^{-1} - 0{,}115 * \mathrm{OM}^{-1} - 0{,}4129 * \ln(\mathrm{OM}) - 0{,}0721 * \rho\mathrm{d} * \mathrm{CS}$$

$$\lambda = 0{,}797 - 0{,}591 * \mathrm{OM} + 0{,}0677 * \mathrm{OM}^2 + 0{,}573 * \mathrm{subsoil}$$

$$\Theta_s = -13{,}6 - 0{,}01533 * CS + 0{,}0000836 * CS^2 - 0{,}0973 * CS^{-1} + 0{,}708 * \rho\mathrm{d}^{-1} - 0{,}00703 * M50 + 225{,}3 * M50^{-1} + 2{,}614 * \ln(M50) + 0{,}0084 * OM^{-1} + 0{,}02256 * \ln(OM) + 0{,}00718 * \rho\mathrm{d} * CS$$

With:

ρ_d = Dry bulk density (g/cm3)

OM = Organic matter content (%)

CS = Clay and silt content (%)

M50 = Median sand particle size (μm)

Topsoil = In case of a A horizon value is 1, for B and C horizons the value is 0.

Subsoil = In case of a A horizon value is 0, for B and C horizons the value is 1.

2.5 Modelling plant growth and irrigation requirement

The SWAP model was used to simulate yield reduction and irrigation requirement caused by drought. Yield reduction were derived from SWAP by taking the ratio between actual and potential transpiration, which can be assumed to be more or less equal to the ratio between actual and potential crop yields *(Moene & van Dam, 2014)*. The reduction of transpiration caused by drought is given by SWAP and was used as an indicator for irrigation requirements. Growth and irrigation reduction were simulated for the 12 different sample locations for a time series of 25 years (1986 – 2011).

2.5.1 The SWAP model

The SWAP model is developed by the university of Wageningen to simulate water, solute and heat transport in the unsaturated part of the soil *(Kroes et al., 2008).* The model is one dimensional and can be used to model vertical fluxes of water, solute and heat that take place between the shallow groundwater at the bottom and the atmosphere (above the canopy) at the top. In horizontal directions the model is most suitable at field scale *(Kroes et al., 2008)*. With the SWAP model it is possible to simulate the potential biomass production, limited by water and/or salinity stresses *(Eitzinger et al., 2004)*.

2.5.2 Climate series

Daily climate records collected by a weather station in Eindhoven operated by the KNMI (Dutch Royal Meteorological Institute) were used as input for the model. This weather station is located about 21 km east-northeast from the research field and a complete dataset was available from 1985 – 2011. The first year (1985) was used to reach hydrostatic equilibrium of the soil moisture head with the Groundwater table so 25 years were left for the simulation.

Makkink formula was used to derive evapotranspiration from meteorological data. This formula was used because it requires only a limited amount of data compared to other equations, which also require data about air humidity, wind velocity and net radiation *(Moene & Van Dam, 2010)*. The Makkink formula is given below *(De Bruin, 1987).*

$$L_vE = 0.65\frac{s}{s+y}\,K\downarrow$$

With:

L_vE = *Latent heatflux*

s = *psychrometer constant (kPa °C-1)*

y = *slope of saturated vapour pressure curve (kPa °C-1)*

$K\downarrow$ = *incoming shortwave radiation*

2.5.3 Lower boundary conditions

During fieldwork in January groundwater was found at location 2 (Figure 5) around -110cm below field level. Because the study was performed at field scale it was assumed groundwater levels are horizontal. Therefore depth of the groundwater level at different locations was determined form the groundwater level at location 2 but corrected for height differences within the field.

No data about changes in groundwater level during the year were available. It was assumed that groundwater table in summer are of lower importance because of the low groundwater tables and coarse sandy soils that do not allow for significant capillary rise in summer *(personal communication Van Dam, 2014)*. Therefore it was roughly estimated that groundwater levels at location 2 gradually decreases from -110 cm at the 1st of March until -150 at the 1st June and towards -198 cm at the 1st of

September. From 1 September to 1 January it is assumed to linearly increase to -110 from which it stays constant until 1 March.

2.5.4 Crop data

A simple pre-defined crop model was used to model the growth of potatoes, no crop rotation was implemented. The pre-defined crop model was slightly adjusted by using crop factors described by Feddes et al. (1987). Feddes described crop factors for particular crops for different moments in year. Because crop factors in SWAP are connected to the Development Stage (DVS), the moments in year used by Feddes had to be translated into a specific DVS number. This was done by taking the average DVS for a specific period, this average DVS was then connected to the crop factor described by Feddes (Table 1). Crop factors were then automatically interpolated for other DVS values. In case no potatoes were grown bare soil with a crop factor 0.5 was assumed.

Table 1 Crop factors during different periods and corresponding development stages used in SWAP. Crop factors derived from Feddes et al., 1987

Period	Soil cover	Crop Factor	Development stage
< - 10 May	Bare soil	0,5	0,00
11 - 20 May	Potatoes	0,7	0,07
21 - 31 May	Potatoes	0,9	0,18
1 - 10 June	Potatoes	1	0,32
11 - 20 June	Potatoes	1,2	0,43
21 - 30 June	Potatoes	1,2	0,55
1 - 10 July	Potatoes	1,2	0,67
11 - 20 July	Potatoes	1,1	0,79
21 - 31 July	Potatoes	1,1	0,91
1 - 10 Aug	Potatoes	1,1	1,04
11 - 20 Aug	Potatoes	1,1	1,16
21 - 31 Aug	Potatoes	1,1	1,28
1 - 10 Sep	Potatoes	0,7	1,41
11 - 20 Sep	Potatoes	0,5	1,53
21 - 30 Sep	Potatoes	0,5	1,65
1 Okt - 31 Dec	Bare soil	0,5	2,00

2.5.5 Soil characteristics

Three functional horizons were distinguished for modeling. Ap, A and C horizon. Variation in depth of the different horizons between the different locations as well as variation in soil hydraulic characteristics of the A horizon were taken into account. For the Ap and C horizon average values for soil hydraulic characteristics were used. Maximum rooting depths were set at the interface between the A and C horizon. An overview of the different modeled locations and their characteristics are given in Attachment B & C. For every functional horizon and the different A horizons the soil hydraulic parameters were determined. Parameters for the water retention curve were derived from lab experiments while the resulting parameters necessary to describe the hydraulic conductivity function were derived from pedotransfer functions.

3. Results and discussion

3.1 Soil compaction

3.1.1Visual observed compaction

Besides the common Ap and A horizon, an extremely dark and stiff layer was observed at the bottom 5cm of the A horizon at location 11. In the field it was assumed that this horizon would be a different and possibly compacted A horizon. In the remainder of this research this horizon is indicated by A*. Except for location eleven no signs of compacted layers within the A or Ap horizon were observed during the profile pit examination.

3.1.2 Penetration resistance

Penetration resistance as a function of depth was measured for most profile pit locations to indicate presence and depth of soil compaction. Unreliable results were not used and as a result no data about location 1, 3, 5, 11 and 13 is available. One or more threshold values of penetration resistance were exceeded within the A horizon for almost every measured location (**Fout! Verwijzingsbron niet gevonden.**). Only at location 13 none of the thresholds was exceeded within the A-horizon. Depending on the thresholds used, the penetration measurement shows that at least part of the A horizons within the field shows signs of compaction. This holds especially for location 7 and 9, where the highest threshold value was exceeded. This result is in contrast with the soil profile examination, where, except for possible signs of compaction at location 11, no compacted soil layers were identified. It should be mentioned however, that penetration measurements are not a very reliable indicator for soil compaction *(Spoor et al., 2003).* They are sensitive for spatial difference like the presence of stones and cracks or different soil moisture content that might influence the penetration resistance.

3.1.3 Dry bulk density

Dry bulk densities were measured to quantify the degree of soil compaction and to determine soil hydraulic characteristics of the different soil layers with use of pedotransfer functions. Highest bulk densities were measured in the natural compacted C horizon. At two locations, bulk density of this horizon was measured with an average of 1.60 g/cm^3, which is exactly the threshold value for soil compaction at sandy soils *(Van den Akker & De Groot 2007)*.

Bulk densities of the Ap horizon are lower with an average of 1.13 g/cm^3. A*, the horizon at the interface of the A and C horizon at location 11 has a bulk density 1.32 g/cm^3, which is below the threshold value for soil compaction. Except for a relatively low dry bulk density at location 13, dry bulk density of the A horizons did not vary much between the locations (Figure 6). At every location the dry bulk density of the A horizon was just below the threshold for soil compaction. But it should be remarked that the samples used to measure dry bulk density were taken at the top of the A horizon. This might result in underestimating the dry bulk density as the penetration measurements showed increasing penetration resistances with depth. Measured bulk densities therefore, do most likely not represent the most compacted part of the A horizons.

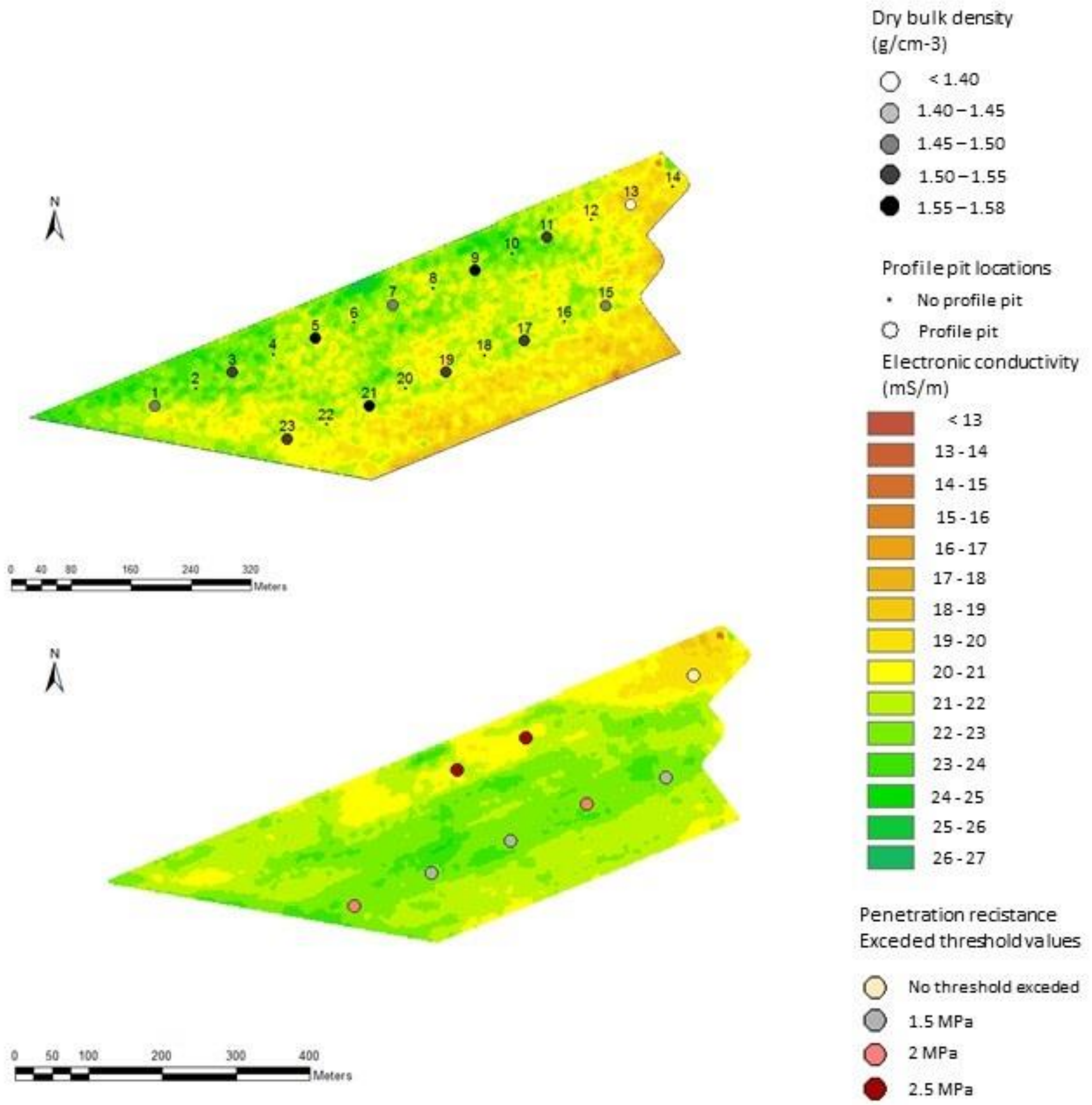

Figure 6, Measured bulk densities at top of the A horizon, just below the interface with the Ap horizon (top). Exceedance of indicated threshold values at 10 cm or more above the interface between the A and C horizon (bottom).

3.1.4 Presence of soil compaction

Evidence for the presence of soil compaction within the field was not univocal and could only be proved by the results of the penetration measurements. Signs for soil compaction were strongest at location 7 and location 9, the only locations were the highest threshold value of 2.5 MPa penetration resistance was exceeded within the A horizon. Therefore these two locations were chosen as being most representative for being affected by soil compaction.

3.2 other soil parameters that may influence hydraulic properties

3.2.1 Electronic conductivity scans

Field scans of the electronic conductivity (EC) were performed at 2 different depths. The results were compared with measurement results of soil texture and soil compaction. Although electronic conductivity scans were performed at different dates only the electronic conductivity scans performed on the 6th of February were used for this research. Scans performed at other dates were either too much influenced by weather phenomena or they showed other signs of high inaccuracy. A rain event influenced the scan performed on the 11th of January as it changed soil moisture contents while the scan was performed. On the 31st of January a frozen layer was present at the start of the measurement but melted away during the scan. Local differences in the melting process lead to spatial and temporal differences. The results were consequently less favourable to determine soil compaction since the artefact of ice in the ground would lead to wrong conclusions.

For the data, derived on 6th of February, spatial patterns can be recognised for measured electronic conductivity at 0-40 cm depth as well as at 0-90 cm depth. At the 0-40 cm depth range, relatively low values for electronic conductivity were measured in the northeastern corner of the field (Figure 7). Measured electronic conductivity at the 0-90 cm depth range showed a different pattern with relatively low electronic conductivity values at the eastern and south eastern side of the field (Figure 7). When measured electronic conductivity are compared with altitude levels some of the areas with higher electronic conductivity values correspond with local altitude minima. This may be explained by increased moisture contents at places were the altitude is low compared to its surrounding.

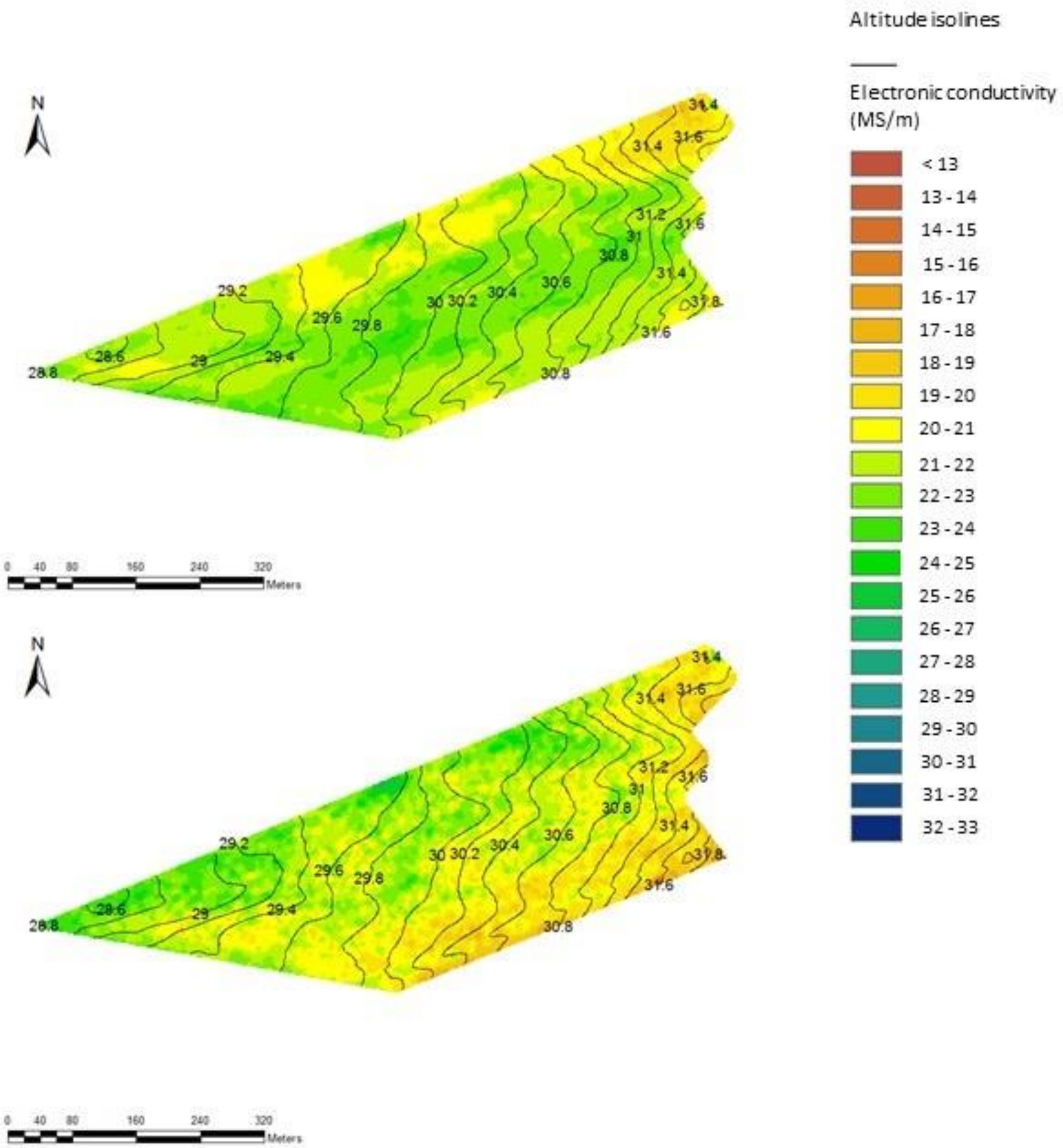

Figure 7, Electrical conductivity at 0-40 cm depth (top) and 0-90 cm depth (bottom) and surface altitude levels measured with EM-38 electronic conductivity sensor

3.2.2 Soil profile

Depths of different horizons were observed visually based on the colour of the soil. At every location a black coloured A horizon on top of a lighter coloured coarse sandy C horizon was observed.

At locations 13, 17, 19, 21 and 23 a podzol B horizon was observed (Figure 9). The presence of a podzol B-horizon is in agreement with information given by the soil map (see section 2.1.2). Characteristics of a podzol B horizon within the C horizon were sometimes very clear with presence of hydro-fibers which makes classification as podzol B horizon very feasible. Though, as the research mainly focused on soil compaction within the A horizon and evidence for podzol B horizon was only found at a few locations, depth of the interface between the podzol B horizon and C horizon was not measured and B horizon was taken as part of the C horizon.

Within the A horizon, differences in compactness were visible. For every location an increase in compactness could be observed around 15-20 cm depth. It was assumed that the increase in compaction between 15 and 20 cm was the result of ploughing as it occurred at a constant depth at every sample location. The upper part of the A horizon was therefore indicated as Ap horizon while the other part is indicated as A horizon. Therefore for every location at least three layers, an Ap, A and C horizon, could be distinguished (Figure 8).

Depth of the interface between the A and the C horizon varied between 30 and 50 cm below soil surface (Figure 9). Deepest A horizons were found at locations were no characteristic podzol horizons were observed, while locations with podzol layers had more shallow A horizons (Figure 9).

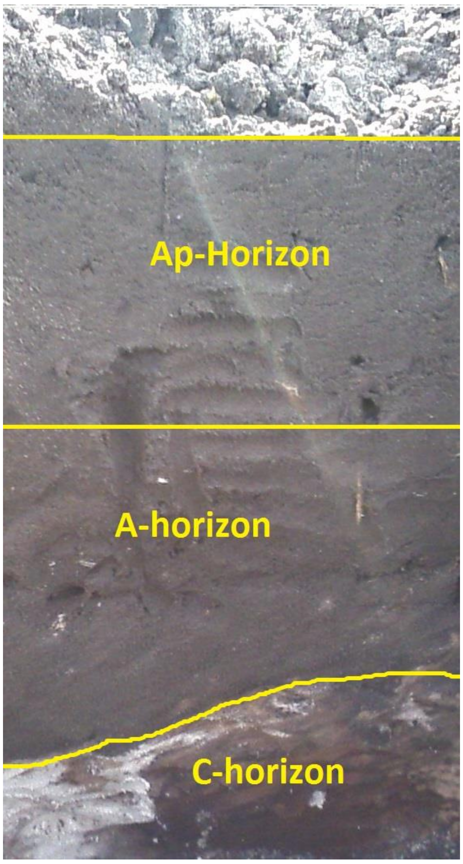

Figure 8, Example of a typical soil profile at the experimental field

3.2.3 Organic matter contents

Organic Matter contents were analysed to support the soil profile observations and for the determination of soil hydraulic functions with pedotransfer functions. The samples of the mixed A and Ap horizon showed clearly higher organic matter contents (Figure 9) than samples taken from the C horizon (Attachment D). Measured organic matter contents are in agreement with reference values from literature *(Wösten et al., 1995)*. The special A horizon (indicated with A*) at location 11 showed a remarkably low organic matter content (0.51%), which is even below the organic matter contents of most C horizons. This indicates that the A* horizon, despite its dark colour, cannot be identified as a special type of A horizon but should rather be indicated as a special layer within the C horizon.

3.2.4 Median grain size and Clay and Silt percentages

Median grain size of sand particles was measured for every horizon at every location. Median grain size of the A horizon at different locations was in the 210-300 µm class, though it was often uncertain whether or not it was more close to the 300-420 µm class. For the C horizon median grain size was categorized as 300 – 420 µm at every location but also here it was often questionable whether it would have been better categorized as 210-300 µm. Because both horizons have the same mother material (cover sands) it was decided to take the grain size as uniform for the whole soil profile and put it at 300 µm.

Clay and Silt percentages of both the A and C horizon were determined separately by taking a random sample out of all locations. For the combined A and Ap horizon a Clay and Silt percentage of 3.1% was determined and for the C horizon a Clay and Silt percentage of 1.7%. It should be noticed that these values might not be good estimates for average clay silt percentages in the field because they are only based on 1, for the C horizon, or 2, in case of the A horizon, locations.

3.2.5 Overview spatial variability

Based on the results described above, the profile pits can be stratified into different groups. From these groups, different locations that represent specific combinations of soil characteristics were selected. This was done in order to be able to better present the results in section 3.3 and 3.4.
First of all there are the profile pits L1 - L11, located along the long north-western side of the field. At these locations no podzol layers were found and EC values between 0 and 90cm depth were relatively high and the A horizon relatively deep compared to other locations. At location L15 – L23, on the other hand, podzols were found (except for location 15) and values for both the depth of the A horizon as well as the Electronic Conductivity at 0-90cm were on average lower. The area around location L13 showed some special characteristics, with a deep A horizon in combination with a podzol and Electronic conductivity values at 0-40 cm depth that were relatively low compared to other locations.

As mentioned in 3.1.4 a possible presence of soil compaction was suggested by penetration resistances that exceeded threshold values for soil compaction at most measurement locations. Highest penetration resistances were measured at location 7 and 9, which indicates that these are the locations within the field with the highest degree of soil compaction. Location 9 was selected as most representative for compacted areas because it has a higher dry bulk density compared to location 7. Other characteristics of location 9 are a relatively deep A horizon, no observed podzol characteristics and a relatively high organic matter content.

Location 13 on the other hand was the only location were the lowest threshold value for soil compaction (1.5MPa) was not exceeded within the A horizon. Therefore and because of its deep A horizon location 13 was selected as most representative for areas with a deep A horizon but no signs of soil compaction. Other characteristics of location 13 are observed podzol characteristics and a high organic matter content.

In order to investigate the effect of the depth of the A horizon location 21 was selected as most representative for areas with a shallow A horizon because together with location 19 it has the shallowest A horizon of all measured locations. Compared to location 19 the organic matter content of location 21 was closer to the organic matter content of location 9 and location 13 which made a comparison between those three more easy. Location 5 was selected to represent locations with a low organic matter content, as it has the lowest organic matter content from all locations.

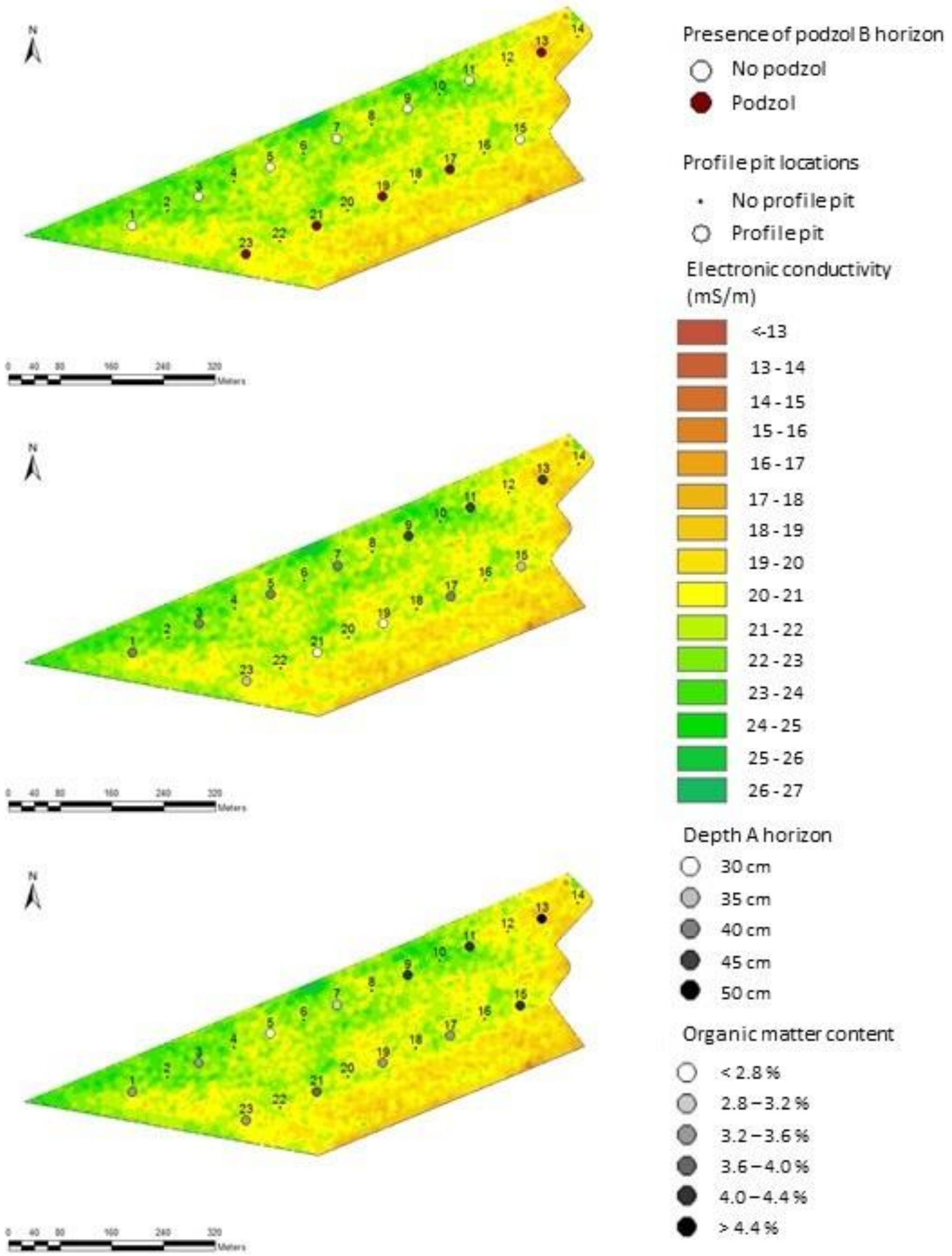

Figure 9, Presence of podzol B-horizon (top). Depth of the A horizon (middle). Organic matter content of the A-horizon (bottom)

3.3 Soil hydraulic properties

3.3.1 Moisture retention

Moisture retention at different pF values was determined in the lab. Curve fitting was used to get water retention functions for the different horizons and every location. In relation to relative transpiration the moisture retention values when the field is at field capacity or dryer (pF > 2) are most important. Clear differences between the average water retention curves of three functional horizons were found (Figure 10). At comparable pF value the C horizon in general contained less moisture compared to the A horizon. Shape of the water retention curve of Ap horizon is totally different from shape of the A horizon with higher moisture contents at saturation and lower moisture contents at pF values just below field capacity (pF=2).

Also for the A horizon itself, there were notable differences in the shapes of derived water retention curves between locations. The A horizon of location 9, which represents the compacted soils, has the highest moisture content of all measured A horizons when the soil is at and just below field capacity (Figure 11). This is in contrast to the low water retention of the A horizon of locations L5 and L13 that represent locations with respectively low organic matter content and uncompact soils. The fitted moisture retention curve of location L13 was relatively high compared to other locations for pF values above 2.4. It should be noticed that for location 13 it was difficult to fit the water retention curve properly. Because of this, the water retention at this location was overestimated for pF values around pF = 3 (Attachment E). The water retention at location 13 measured in the lab for pF = 3 was around 0.025, which is comparable to the water retention of other representative A horizons.

When the inaccuracy by curve fitting is taken into account, water retention values at or below field capacity are generally lowest for the locations L5 and L13, with respectively low organic matter contents and low degree of soil compaction. The A horizons of location 9 and 13 mainly differed in the degree of compaction observed, without a lot of variation in other measured and observed characteristics. Differences in water retention between these locations can therefore be subscribed to differences in soil compaction. These results suggest that both the degree of compaction and the organic matter content influence water retention. Higher organic matter content as well as a higher degree of soil compaction could be related to increased water retention.

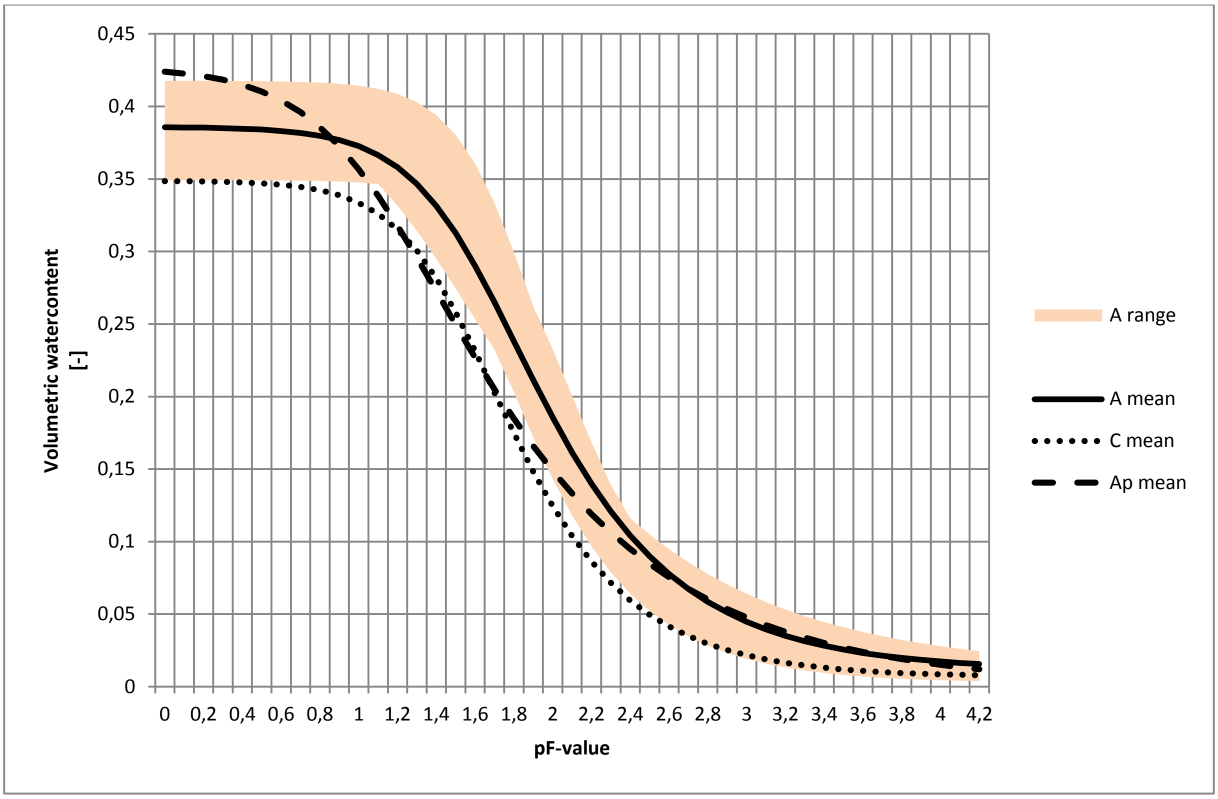

Figure 10, Average water retention curves of the three functional horizons derived from lab measurements by curve fitting.

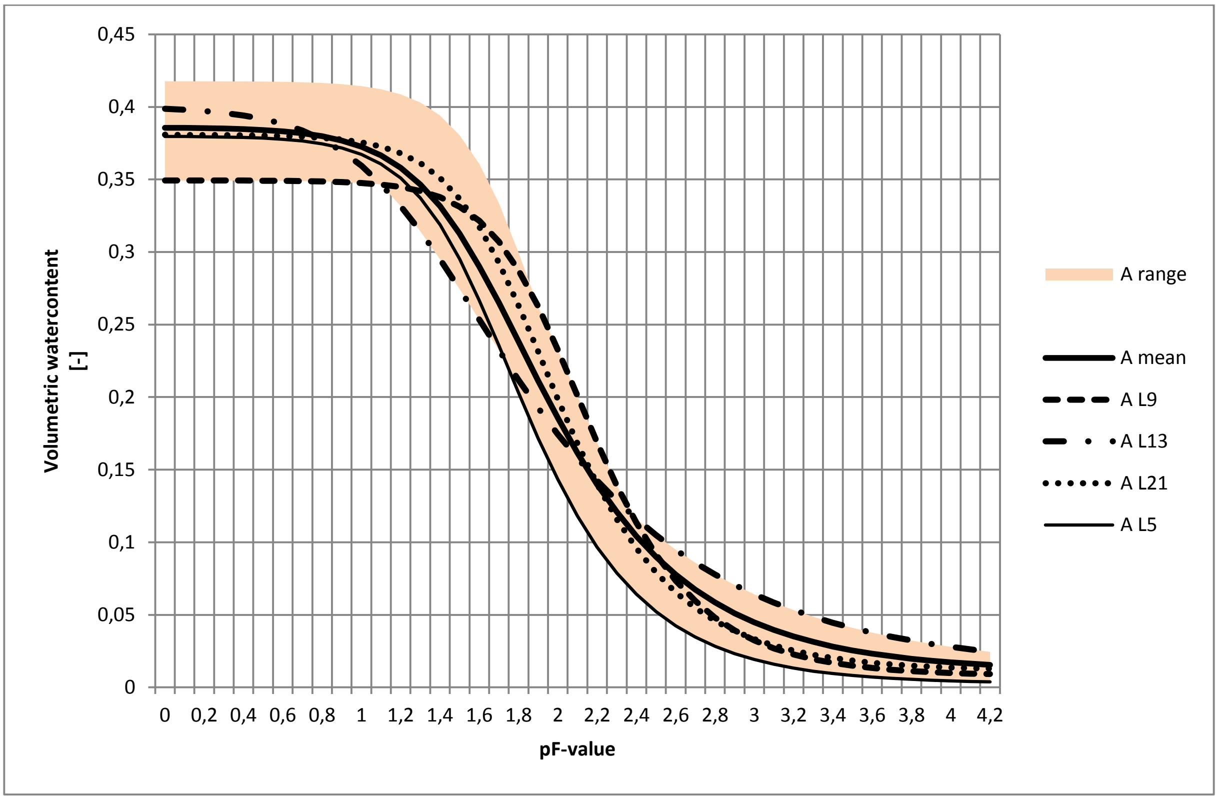

Figure 11, Water retention curves of the A horizon at different representative locations compared to the range of water retention curves found at all profile pit locations. Location 9 represents locations with a deep A and compacted horizon, location 13 a deep compacted A horizon, location 21 a shallow average compacted A horizon and location 5 represents locations with a deep A horizon but low organic matter content.

3.3.2 Hydraulic conductivity

Parameters used to describe the water retention curves were also used to describe the conductivity functions, except for the saturated conductivity and shape parameter λ, which cannot be derived from water retention curves. Instead these parameters were derived with use of pedotransfer functions. Clear differences between the hydraulic conductivity curves of three functional horizons were found (Figure 12). At field capacity the C horizon already has a low hydraulic conductivity, with a relatively steep decline when the soil dries out.

Also for the A horizon itself, there were notable differences in hydraulic conductivity. Highest hydraulic conductivities were found for the A horizon at location L9, representing the most compacted soil (Figure 13). Lowest values for hydraulic conductivity were found for the A horizon at location L13 and location L5, representing respectively soils without compaction and soils with a low organic matter content (Figure 13). These results suggest that both organic matter content and soil compaction influence the hydraulic conductivity of a soil. Both soil characteristics have the potential to increase hydraulic conductivity of the soil. At field capacity hydraulic conductivity was almost mainly explained by differences in the degree of soil compaction, which was also noticed in the water retention curves. At higher pF values it was mainly explained by differences in organic matter content.

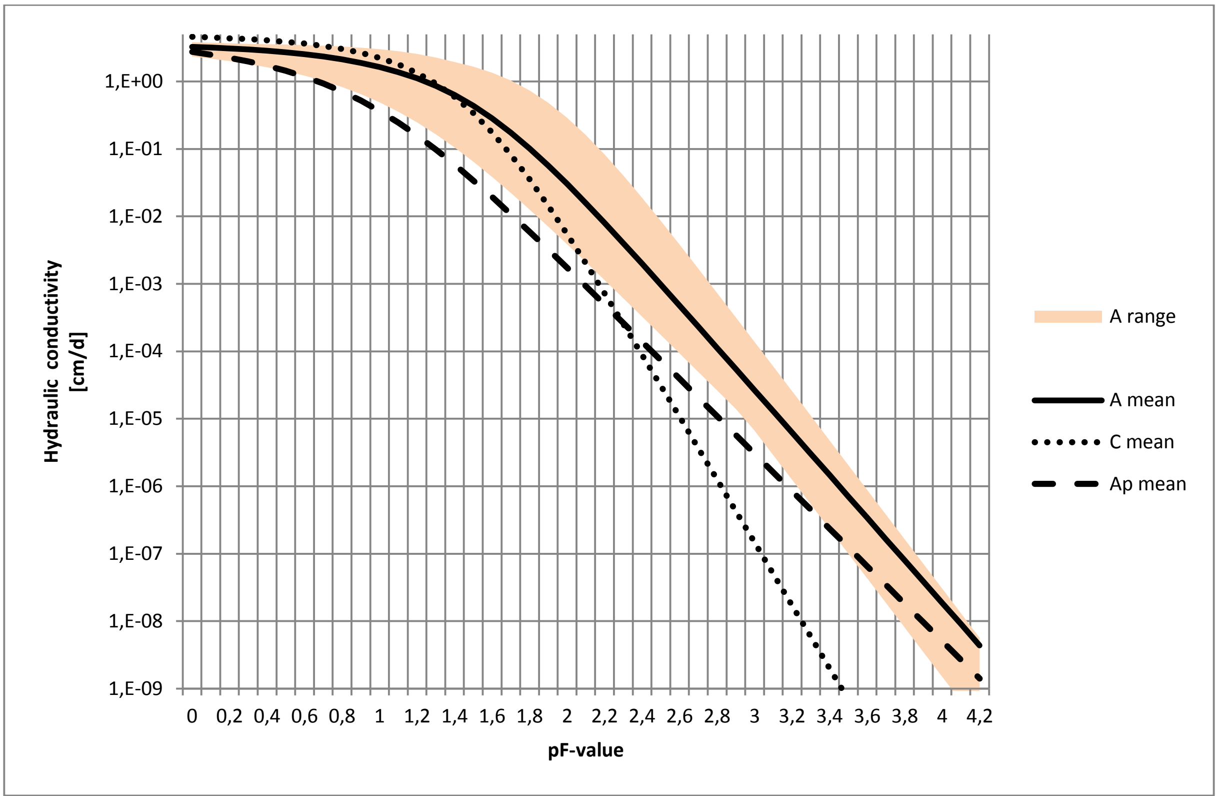

Figure 12, Average hydraulic conductivity of 3 functional horizons derived from lab experiments and pedotransfer functions

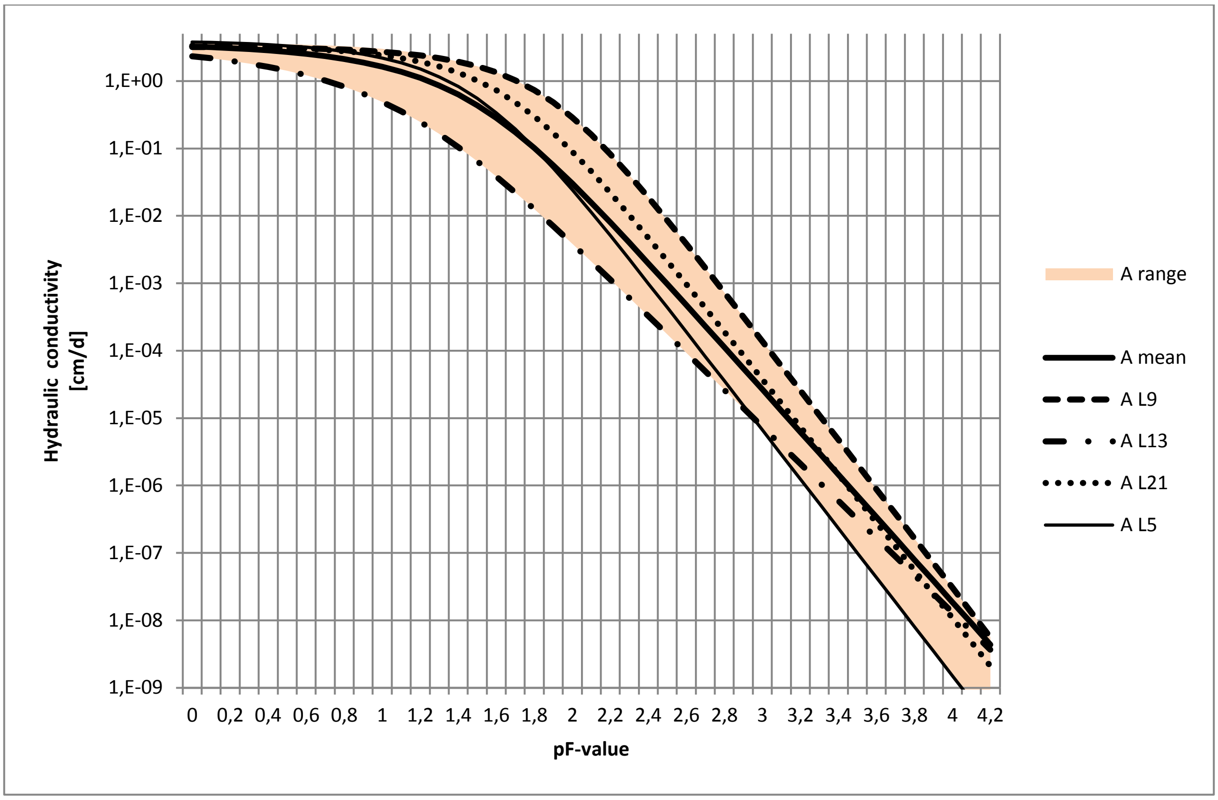

Figure 13, Hydraulic conductivity curves of the A horizon at different representative locations compared to the range of hydraulic conductivity curves found at all profile pit locations. Location 9 represents locations with a deep A and compacted horizon, location 13

3.4 Relative transpiration

Relative transpiration was modelled for all 23 measurement locations. Results are discussed based on 4 representative locations.

Highest values for relative transpiration were calculated for location L9 that represents the compacted soils (Figure 14). Relative transpiration values for location L5, L13 and L21 were relatively low compared to other locations.

Differences in modelled relative transpiration can be explained by difference in the depth of A horizon and differences in its hydraulic characteristics between different locations. Location 9 was characterized by a deep A horizon, and a high hydraulic conductivity and a high water retention of this A horizon. As a result of higher water retention capacity of the soil, there will be more water available for plants and thereby relative transpiration will be higher in times of drought *(Penman, 1948)*.

The low relative transpiration values are linked to a relatively shallow A horizon at location 21 and low values for hydraulic conductivity and water retention in the A horizons of location 5 and 13.

Differences in soil hydraulic characteristics between the A and C horizon in combination with different depths of the A horizons can explain the differences in modelled relative transpiration. For every location both the soil hydraulic conductivity as well as the water retention of the A horizon was higher than the average hydraulic conductivity and water retention of the underlying C horizon. Therefore soils with a deeper A horizon have the potential to retain more water and allow higher speeds of capillary rise.

Because of the deep groundwater tables used for modelling, the relative transpiration and the coarse sandy soils, the effects of capillary rise can be assumed to be negligible *(Personal communication Jos Van Dam)*.

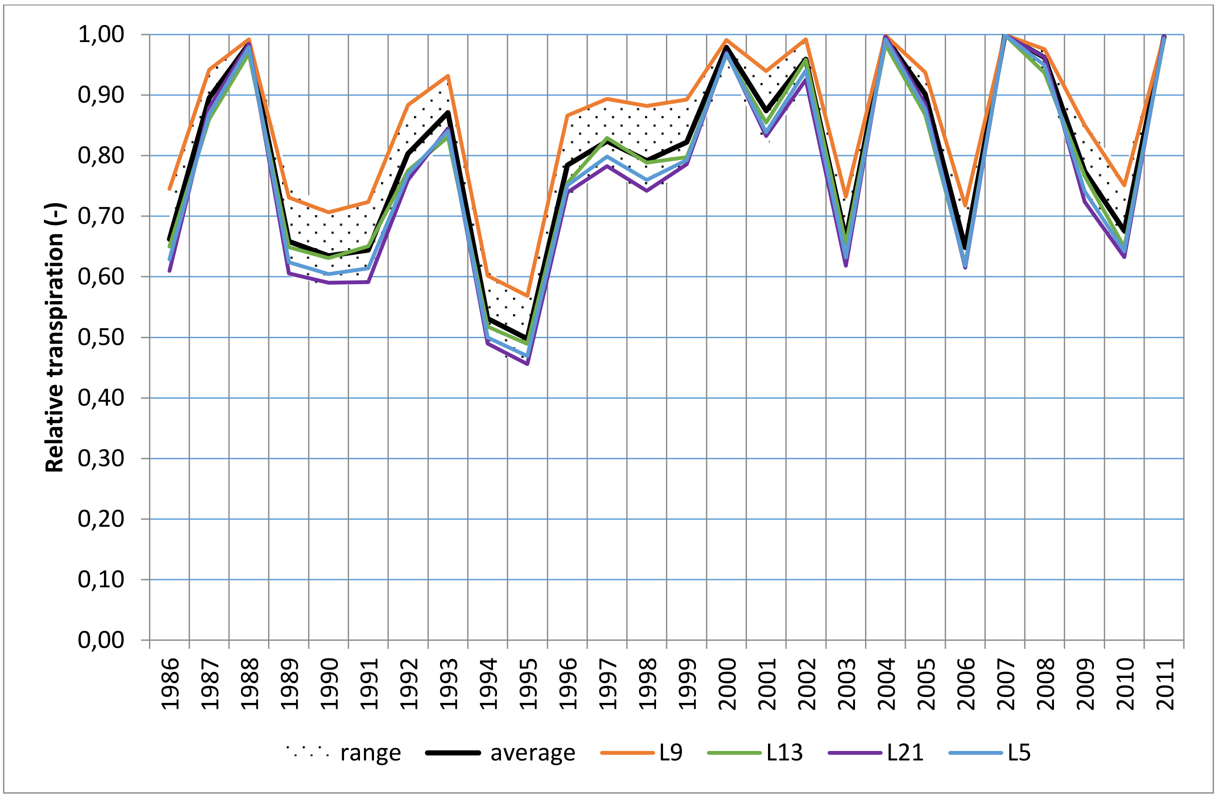

Figure 14, Simulated ratio between actual and potential transpiration for the four representative locations since 1986.

3.5 General assessment of results

3.5.1 Capturing spatial variability of soil profile characteristics

This research was done in a way that spatial variability of most of soil profile characteristics that influence soil hydraulic properties were captured. Though it was impossible to capture spatial variability of every soil profile characteristic in this research.

The Clay and Silt percentages of the A horizon could not be determined for every location, instead an average Silt and Clay content was determined. This had several consequences. First it meant that spatial difference of Silt and Clay content were not taken into account for the determination of some parameters needed to describe the hydraulic conductivity function. Consequences will be described in 3.5.2. Besides this it also means that the influence of spatial differences in Clay and Silt percentage on simulation results could not identified. Therefore it remains unknown whether Clay and Silt percentages might be a hidden variable in the observed influence of soil compaction on plant growth and irrigation requirements.

Also spatial variation of most soil characteristics of the C and Ap horizon were not taken into account. This also implied that soil hydraulic properties were assumed to be equal for every location. As a consequence the results of this research ignore influence of soil compaction and other soil characteristics within the underlying C horizon. This included possible influence of underlying podzol B horizon which were not captured in this research as well.

3.5.2 Determination of soil compaction

Although no compacted soil layers were identified visually within the field, penetrometer measurements suggests presence of over compaction at the bottom of the A horizon at different locations. Unfortunately ring samples to measure bulk density and water retention values were only taken from the top of the A horizon. This might explain why bulk densities did not exceed threshold values for compaction. But it also implicated that neither the presence of soil compaction indicated by values of penetration resistance nor the absence of soil compaction observed by profile observations could be supported by bulk densities. As a result it remains unclear whether soil compaction was present within this field. Besides this, the depth of sampling also influenced determination of soil hydraulic properties, which will be discussed in the next section.

3.5.3 Determination of soil hydraulic properties

Soil hydraulic properties were determined by a combination of lab measurements, curve fitting and pedotransfer functions. Samples used for lab experiments were taken from the top of the A horizon where no signs of soil compaction were found and therefore might not be representative for the A horizon as a whole and also less appropriate for describing the effects of soil compaction. The question remains whether the use of samples from deeper parts of the A horizon would have led to comparable results.

Use of curve fitting could also be a source for errors. Especially water retention values at pF=3 for the A horizon of location 13 could not be described well by curve fitting. As a result water retention and probably also hydraulic conductivity at low pF values were overestimated by fitted curves, which were subsequently used in SWAP. Though it should be mentioned that this probably might have only minor impacts as the modelling results were mainly influenced by water retention values around field capacity.

Pedotransfer functions were only used to determine saturated hydraulic conductivity and the shape parameter λ for the soil hydraulic conductivity function because these parameters were not derived in the lab. In a comparison between water retention curves derived from the lab experiments and the ones derived from pedotransfer functions big differences are visible for the Ap horizon (Figure 15). Therefore it can be assumed that the soil hydraulic conductivity functions show some extra uncertainty caused by errors in the calculation of shape parameter λ and saturated hydraulic conductivity on top of uncertainty already caused by errors in lab experiments and curve fitting. However, it should be mentioned that differences in modelling outcome between different locations are probably mainly caused by differences in water retention at the start of the growing season. Therefore the influence of the soil hydraulic conductivity and underlying errors on the modelling results can be assumed to be relatively small.

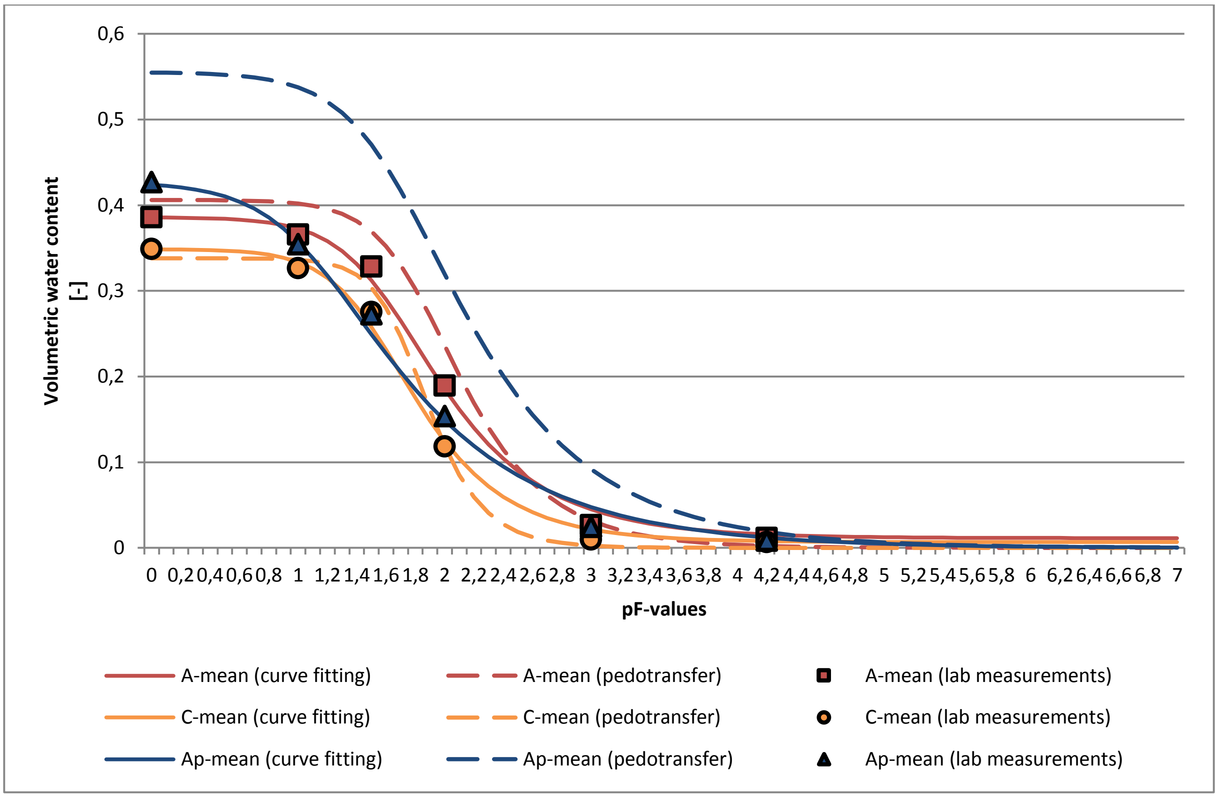

Figure 15, Comparison of water retention curves derived by pedotransfer fucntions and derived by curve fitting based on lab results.

3.5.4 Simulation in SWAP

Groundwater levels were based on an estimated groundwater level at location 2 at the 31st of January, and corrected for differences in surface elevation level. Because of this estimation based on one location there is an uncertainty in the groundwater levels used for the simulation. An extra simulation with different constant groundwater tables was performed for the three most important locations to see the effect of inaccuracy in groundwater tables on the reduction of transpiration by drought (Figure 16). Differences in absolute reduction of transpiration by drought were found, though no effect on the relative differences between different locations. This proves that relative differences in modeled relative transpiration between different locations are not influenced by the height of the groundwater tabel.

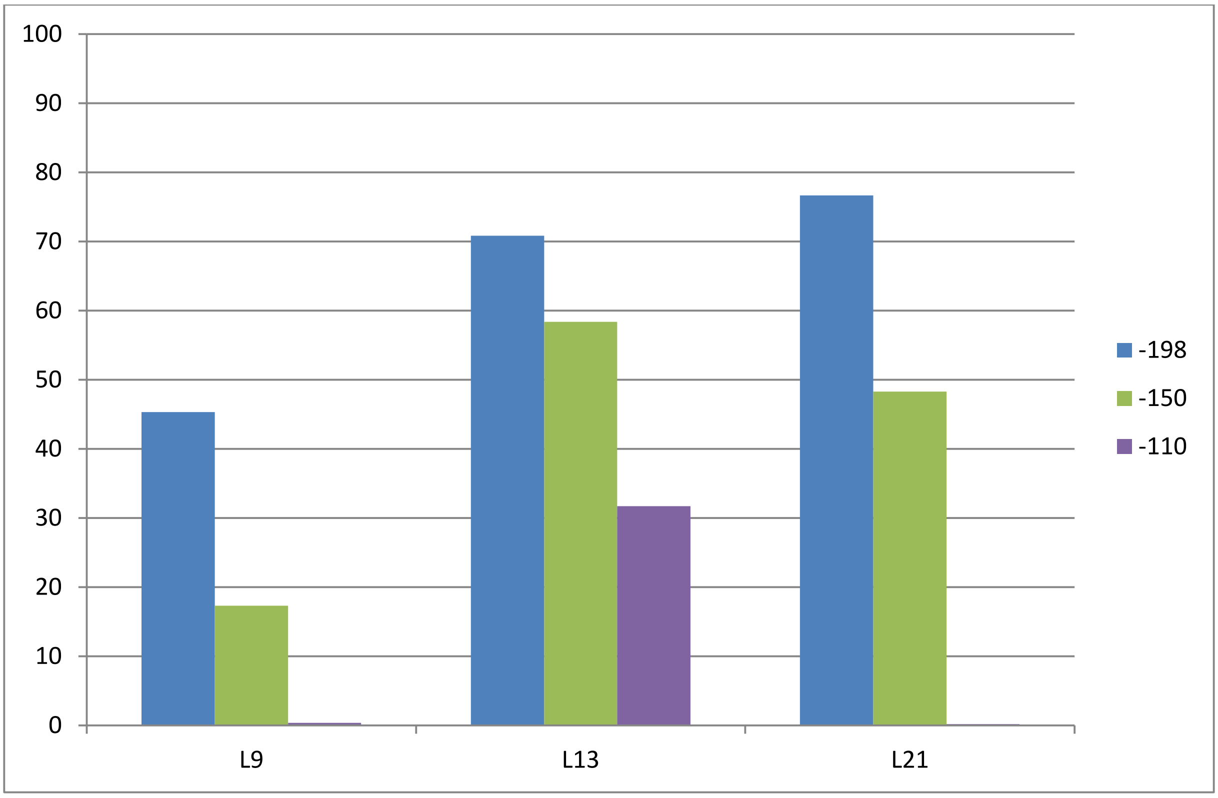

Figure 16, Simulated reduction of transpiration by drought for three different representative location in July 1995 for different constant groundwater tables.

4. Conclusions & Recommendations

Presence of human induced over compaction at the research location could not be proofed by visual observation or by bulk densities. Signs of human induced soil compaction were only found in the form of penetration resistances that exceeded threshold values for soil compaction within the A horizon. Results of the simulations suggest that differences in relative transpiration can be explained by differences in the water retention capacity of the soil. The water retention capacity of the soil profile could be related to differences in the depth of the A horizon, the degree of compaction and organic matter content.

The effect of soil compaction could be compared quite well with the effect of other soil variables by assignment of representative locations. Highest values for relative transpirations were found at the location that was characterized by showing the strongest signs of compaction and a relatively thick A horizon that was high in organic matter. Lowest values for relative transpiration were found at locations that were either having no signs of compaction, low organic matter contents or a shallow A horizon.

From this research it can be concluded that moisture delivery capacity of a sandy soil with a deep groundwater table is increased by the presence of a deep A horizon with a high water retention capacity. The research also suggests that the water retention capacity of the soil can be improved by increased organic matter content or by higher degree of compaction. Though it should be mentioned that measured bulk densities were still below threshold values for over compaction. The question remains what will happen when soil compaction really exceeds threshold values for over compaction. In those cases it might also decrease rooting depth and therefore decrease accessibility of water and nutrients by plants.

More research is also needed towards the effect of soil compaction for cases in which the soil shows signs of over compaction and in which threshold values are exceeded. For the field where the research was performed, penetrometer measurements showed evidence for over compaction that were not supported by bulk density measurements and profile pit observations. Therefore measurements of bulk densities and soil hydraulic characteristics at different depths within the A horizon are recommended, also when no compacted layers can be visually observed.

Because of the limited scale of this experiment it is difficult to answer the question on how transpiration data and data about other soil characteristics can be used to detect the presence of soil compaction on a large scale. Still this research shows that its is potential possible to detect area’s with soil compaction with use of relative transpiration data. Next question will be how this can be done in practice and for bigger area’s.

References

Batey, T. (2009). Soil compaction and soil management–a review. Soil Use and Management, 25(4), 335-345.

Batey, T., and McKenzie, D. (2006). Soil compaction: identification directly in the field. Soil Use and Management, 22(2), 123-131.

Blake, G. R. K. H. H. (1986). Bulk density. In A. Klute (Ed.), Methods of soil analysis, part 1; Physical and Mineralogical methods (9 ed., Vol. 9, pp. 363-375). Madison, Wisconsin USA: ASA and SSSA.

Borne, J. V. d. (2013). Van den Borne aardappelen. Retrieved 21 oktober, 2013, from http://www.vandenborneaardappelen.com/301/welkom

CEG. (2006). Thematic Strategy for Soil Protection from the Commission of the European Communities. CEG Retrieved from http://eur-lex.europa.eu/LexUriServ/LexUriServ.do?uri=COM:2006:0231:FIN:EN:PDF.

Cressie, N. (1990). The origins of kriging. Mathematical Geology. 22(3), 239-252. doi: 10.1007/bf00889887

De Bruin, H. A. R. (1987). From Penman to Makkink. Evaporation and Weather, Comm. Hydrol. Res. TNO, Den Hag, Proc. and Inform.,, 39, 5-30.

Edelenbosch, A. (2011). Advies Bodemverdichting aan De Staatssecretaris van Infrastructuur en Milieu. Technische commissie bodem, TCB A071 (2011).

Ehlers, W., and Goss, M. (2003). Water dynamics in plant production. Wallingford: CABI Publishing.

Eitzinger, J., Trnka, M., Hösch, J., Žalud, Z., & Dubrovský, M. (2004). Comparison of CERES, WOFOST and SWAP models in simulating soil water content during growing season under different soil conditions. Ecological Modelling, 171(3), 223-246.

GDI-Vlaanderen (2014). Geodatabase subsurface vlaanderen.

Genuchten, M. T. v. (1980.). A closed form equation for predicting the hydraulic conductivity of unsaturated soils. Soil Sci. Soc. Am. J.,, 44, 892-898.

GEONOMICS LIMITED (2008). EM38-MK2 Ground conductivity meter operating manual. Mississauga, Ontario, Canada: GEONOMICS LIMITED.

Håkansson, I and Reeder, R.C. (1994). Subsoil compaction by vehicles with high axle load-extent, persistence and crop response. Soil and Tillage Research, 29, 277-304.

Hoefer, G., Bachmann, J., & Hartge, K. (2010). Can the EM38 Probe Detect Spatial Patterns of Subsoil Compaction? Proximal Soil Sensing (pp. 265-273): Springer.

Howard, P., & Howard, D. (1990). Use of organic carbon and loss-on-ignition to estimate soil organic matter in different soil types and horizons. Biology and Fertility of soils, 9(4), 306-310.

Howard, P. J. A. (1965). The Carbon-Organic Matter Factor in Various Soil Types. Oikos, 15(2), 229-236. doi: 10.2307/3565121

Klute, A. (1986). Water retention: laboratory methods. In A. Klute (Ed.), Methods of soil analysis; Part 1; Physical and Mineralogical methods (pp. 635-662). Madison, Wisconsin: ASA and SSSA.

Kooistra, L. (2011). Verificatie remote versus near sensing voor toepassingen in precisielandbouw. PPL project (Vol. 023).

Kroes, J. G., Van Dam, J.C., Groenendijk, P., Hendriks, R.F.A., Jacobs, C.M.J. (2008). SWAP version 3.2 Theory description and user manual. Alterra-report 1649, ISSN 1566-7197: Alterra.

Lamberink, K. (2013). Exploring subsoil compaction on arable farms in East-Flevoland. (Msc), Wageningen University, Wageningen

Moene, A.F., and Van Dam, J.C. (2010). Course quide: Atmosphere-Vegetation-Soil Interactions.

Moene, A.F., and Van Dam, J.C. (2014). Transport in the Atmosphere-Vegetation-Soil Continuum. Cambridge University Press, New York, 436 p.

Monteith, J.L. (1965). Evaporation and environment. Symposia of the Society for Experimental Biology 19: 205–224

Mualem, Y. (1976). A new model for predicting the hydraulic conductivity of unsaturated porous media. Water Resour. Res., 12, 513-522.

Penman, H.L. (1948) Natural evaporation from open water, bare soil and grass, Proceedings of the Royal Society London, vol. 193 no. 1032 p. 120-145

Reintam, E., Trükmann, K., Kuht, J., Nugis, E., Edesi, L., Astover, A., . . . Rannik, K. (2009). Soil compaction effects on soil bulk density and penetration resistance and growth of spring barley (Hordeum vulgare L.). Acta Agriculturae Scandinavica Section B–Soil and Plant Science, 59(3), 265-272.

Ruijun, M., McBratney, A., Whelan, B., Minasny, B., & Short, M. (2011). Comparing temperature correction models for soil electrical conductivity measurement. Precision agriculture, 12(1), 55-66.

Scott, C. A., Bastiaanssen, W. G., & Ahmad, M.-u.-D. (2003). Mapping root zone soil moisture using remotely sensed optical imagery. Journal of irrigation and drainage engineering, 129(5), 326-335.

Spoor, G., Tijink, F., & Weisskopf, P. (2003). Subsoil compaction: risk, avoidance, identification and alleviation. Soil and Tillage Research, 73(1), 175-182.

Tanner, C.B., and Pelton, W.L. (1960). Potential Evapotranspiration estimates by the approximate energy balance method of Penman, Journal of Geophysical Research, Vol. 65 Nr. 10

Van den Akker, J., Arvidsson, J., & Horn, R. (2003). Introduction to the special issue on experiences with the impact and prevention of subsoil compaction in the European Union. Soil and Tillage Research, 73(1), 1-8.

Van den Akker, J. J., & Hoogland, T. (2011). Comparison of risk assessment methods to determine the subsoil compaction risk of agricultural soils in The Netherlands. Soil and Tillage Research, 114(2), 146-154.

van den Akker, J. J. H., de Groot, W.J.M. (2007). Een inventariserend onderzoek naar de ondergrondverdichting van zandgronden en lichte zavels. Alterra-rapport 1450, ISSN 1566-7197: Alterra.

Vermeulen, G. D., Verwijs, B.R., Akker, J.J.H. van den. (2013). Vergelijking van de bodembelasting bij agrarisch veldwerk in 1980 en 2010 Plant Research International, Wageningen (Vol. Report 501).

Wilcox, A., Perry, N., Boatman, N., & Chaney, K. (2000). Factors affecting the yield of winter cereals in crop margins. The Journal of Agricultural Science, 135(4), 335-346.

Wong, M., Wittwer, K., Oliver, Y., & Robertson, M. (2010). Use of EM38 and gamma ray spectrometry as complementary sensors for high-resolution soil property mapping Proximal soil sensing (pp. 343-349): Springer.

Wösten, J. (1997). Pedotransfer functions to evaluate soil quality. Developments in Soil Science, 25, 221-245.

Wösten, J., Finke, P., & Jansen, M. (1995). Comparison of class and continuous pedotransfer functions to generate soil hydraulic characteristics. Geoderma, 66(3), 227-237.

Young. (2012). Encyclopedia of Soil Science.

Zwart et al. (2011). Notitie 'bodemverdichting en remote sening. Alterra. Cited by Edelenbosch, A. 2011, Advies Bodemverdichting aan De Staatssecretaris van Infrastructuur en Milieu. Technische commissie bodem, TCB A071.

Attachment A Identified soil horizons for the different measurement locations

	Horizon 1		Horizon 2		Horizon 3		Horizon 4	
Location	Depth (cm)	Id	Depth (cm)	Id	Depth (cm)	Id	Depth (cm)	Id
1	0-15	1-Ap	15-40	1-A	-	-	40<	1-C
3	0-20	3-Ap	20-40	3-A	-	-	40<	3-C
5	0-15	5-Ap	15-40	5-A	-	-	40<	5-C
7	0-15	7-Ap	15-40	7-A	-	-	40<	7-C
9	0-20	9-Ap	20-45	9-A	-	-	45<	9-C
11	0-15	11-Ap	15-40	11-A	40-45	11-A*	45<	11-C
13	0-15	13-Ap	15-45	13-A	-	-	45<	13-C
15	0-20	15-Ap	20-35	15-A	-	-	35<	15-C
17	0-20	17-Ap	20-40	17-A	-	-	40<	17-C
19	0-15	19-Ap	15-30	19-A	-	-	30<	19-C
21	0-15	21-Ap	15-30	21-A	-	-	30<	21-C
23	0-15	23-Ap	15-35	23-A	-	-	35<	23-C

Attachment B Modeled locations and their corresponding horizons

		Layer 1		Layer 2		Layer 3	
Run	Location	Horizon	Depth [cm]	Horizon	Depth [cm]	Horizon	Depth [cm]
A	1	Ap-mean	0 - 15	A-1	15 - 40	C-mean	40 - 60
B	3	Ap-mean	0 - 20	A-3	20 - 40	C-mean	40 - 60
C	5	Ap-mean	0 - 15	A-5	15 - 40	C-mean	40 - 60
D	7	Ap-mean	0 - 15	A-7	15 - 40	C-mean	40 - 60
E	9	Ap-mean	0 - 20	A-9	20 - 45	C-mean	45 - 60
F	11	Ap-mean	0 - 15	A-11	15 - 45	C-mean	45 - 60
G	13	Ap-mean	0 - 15	A-13	15 - 45	C-mean	45 - 60
H	15	Ap-mean	0 - 20	A-15	20 -35	C-mean	35 - 60
I	17	Ap-mean	0 - 20	A-17	20 - 40	C-mean	40 - 60
J	19	Ap-mean	0 - 15	A-19	15 - 30	C-mean	30 - 60
K	21	Ap-mean	0 - 15	A-21	15 - 30	C-mean	30 - 60
L	23	Ap-mean	0 - 15	A-23	15 - 35	C-mean	35 - 60

Attachment C Hydraulic parameters for the different horizons

Horizon	n [-]	α [-]	l [-]	θ-res [-]	θ-sat [-]	K-sat
Ap-mean	1.50	0.080	-0.44	0.00E+00	0.43	195.14
A-mean	1.75	0.025	-0.44	1.14E-02	0.39	43.78
C-mean	1.92	0.030	0.84	6.72E-03	0.35	141.65
A-1	1.75	0.025	-0.44	7.84E-03	0.38	46.25
A-3	1.75	0.025	-0.4	1.22E-02	0.39	49.63
A-5	1.96	0.026	-0.28	2.65E-03	0.38	55.61
A-7	1.93	0.026	-0.37	1.31E-02	0.38	59.28
A-9	2.10	0.011	-0.48	7.98E-03	0.35	25.95
A-11	1.95	0.018	-0.47	1.44E-02	0.38	25.64
A-13	1.50	0.054	-0.48	1.12E-02	0.40	51.93
A-15	2.20	0.015	-0.48	1.39E-02	0.42	40.74
A-17	2.00	0.018	-0.43	1.36E-02	0.39	37.38
A-19	2.00	0.016	-0.43	1.23E-02	0.40	42.26
A-21	2.00	0.017	-0.45	1.16E-02	0.38	31.96
A-23	2.00	0.025	-0.43	1.58E-02	0.38	46.20

Attachment D Measured organic matter content

Remark: Except for location L11 organic matter contents of the Ap and A horizon were derived from the same composite samples.

Location	Ap^{-1}	A^{-1}	A*	C
L1	3.54	3.54	-	0.50
L3	3.20	3.20	-	0.66
L5	2.61	2.61	-	0.46
L7	3.05	3.05	-	0.33
L9	4.31	4.31	-	0.36
L11	3.23	4.89	0.51	-
L13	4.45	4.45	-	1.19
L15	4.22	4.22	-	1.05
L17	3.49	3.49	-	1.81
L19	3.43	3.43	-	1.66
L21	3.63	3.63	-	1.13
L23	3.47	3.47	-	0.96
Average	3.57	3.64	0.51	0.96

Attachment E Results of curve fitting for the A horizons of the 4 representative locations

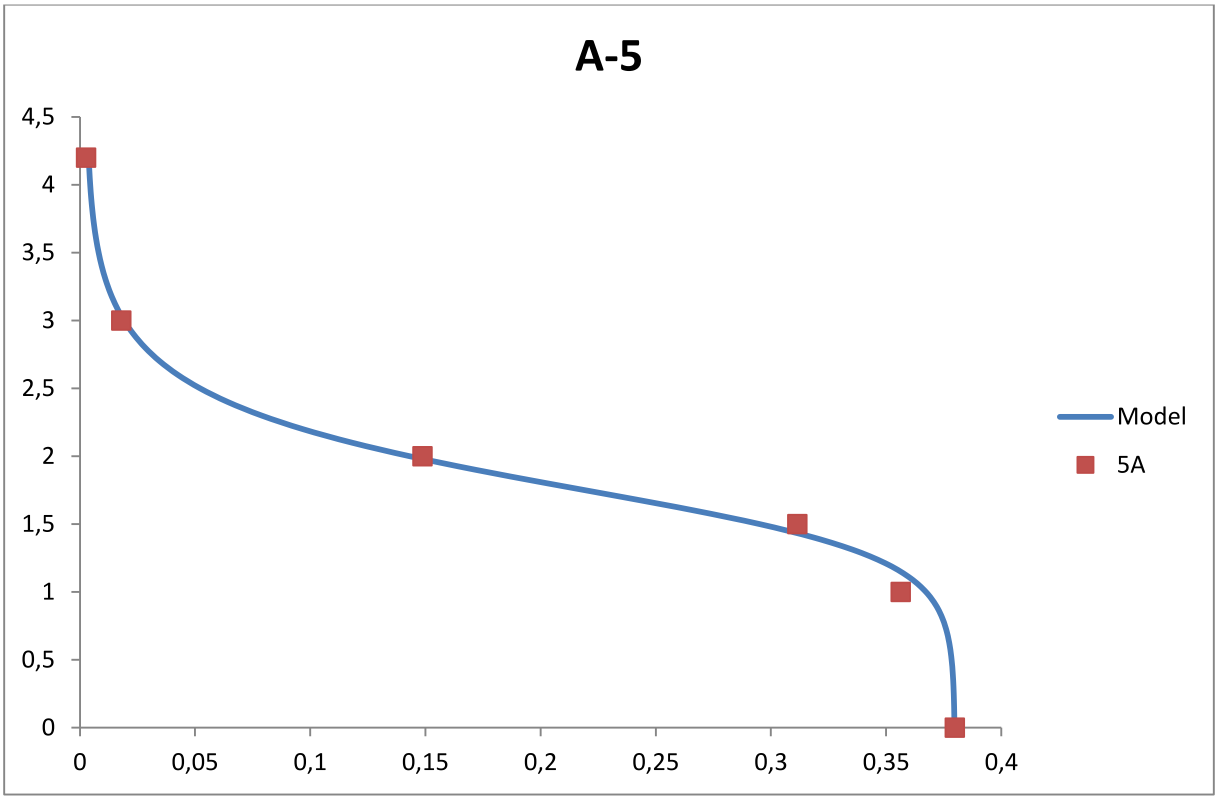

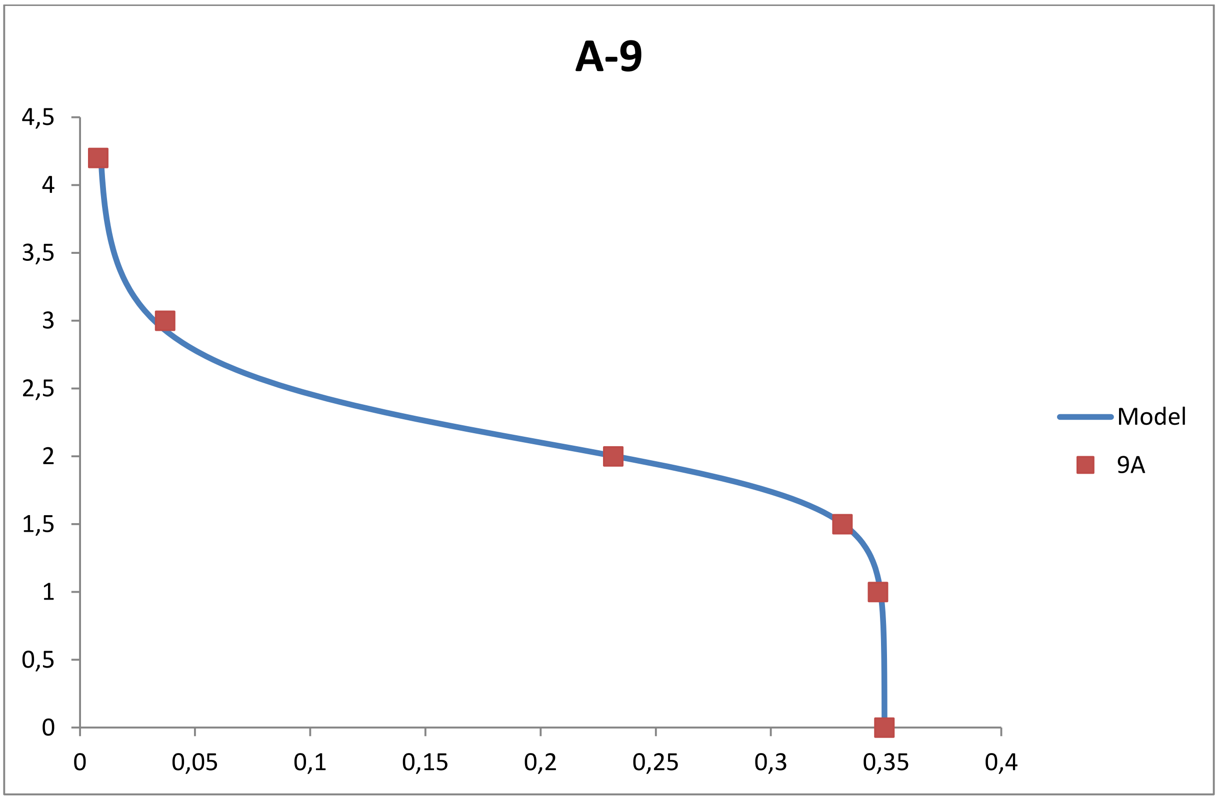

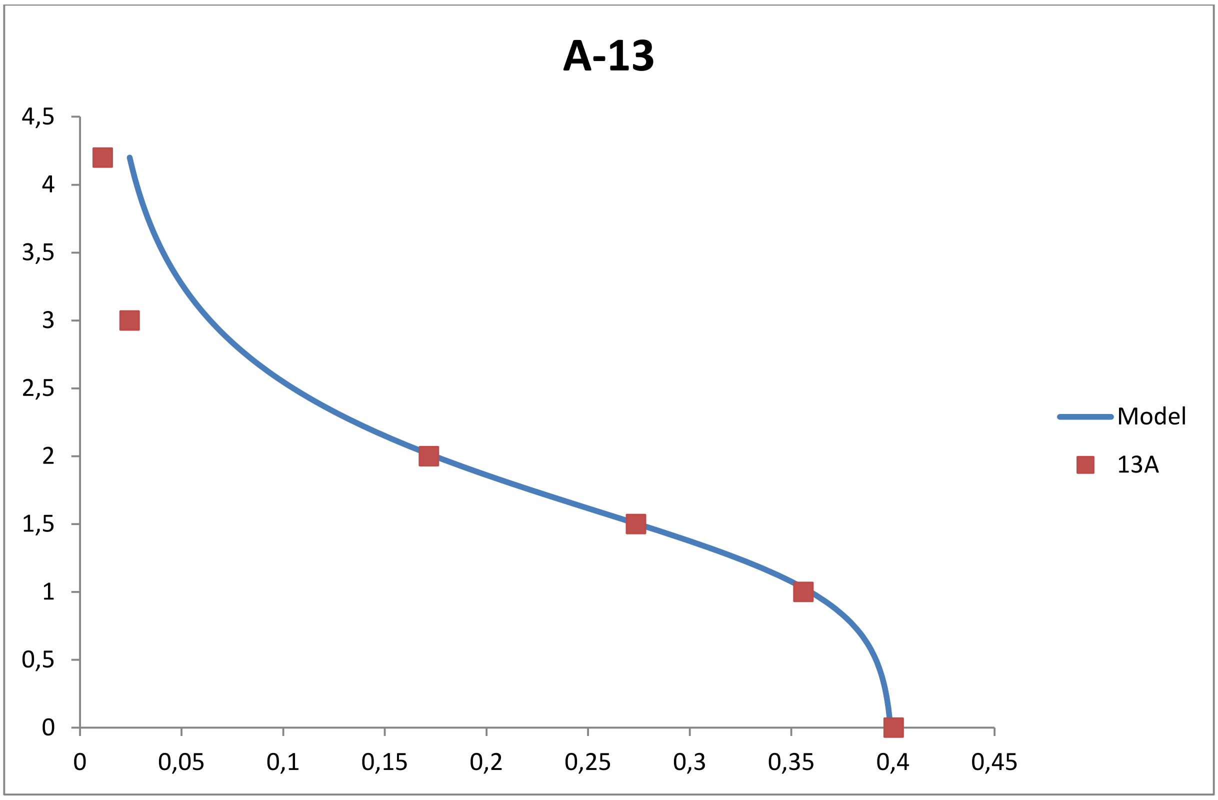

A-13
4,5
4
3,5
3
2,5
2
1,5
1
0,5
0
0
0,05
0,1
0,15
0,2
0,25
0,3
0,35
0,4
0,45
Model
13A

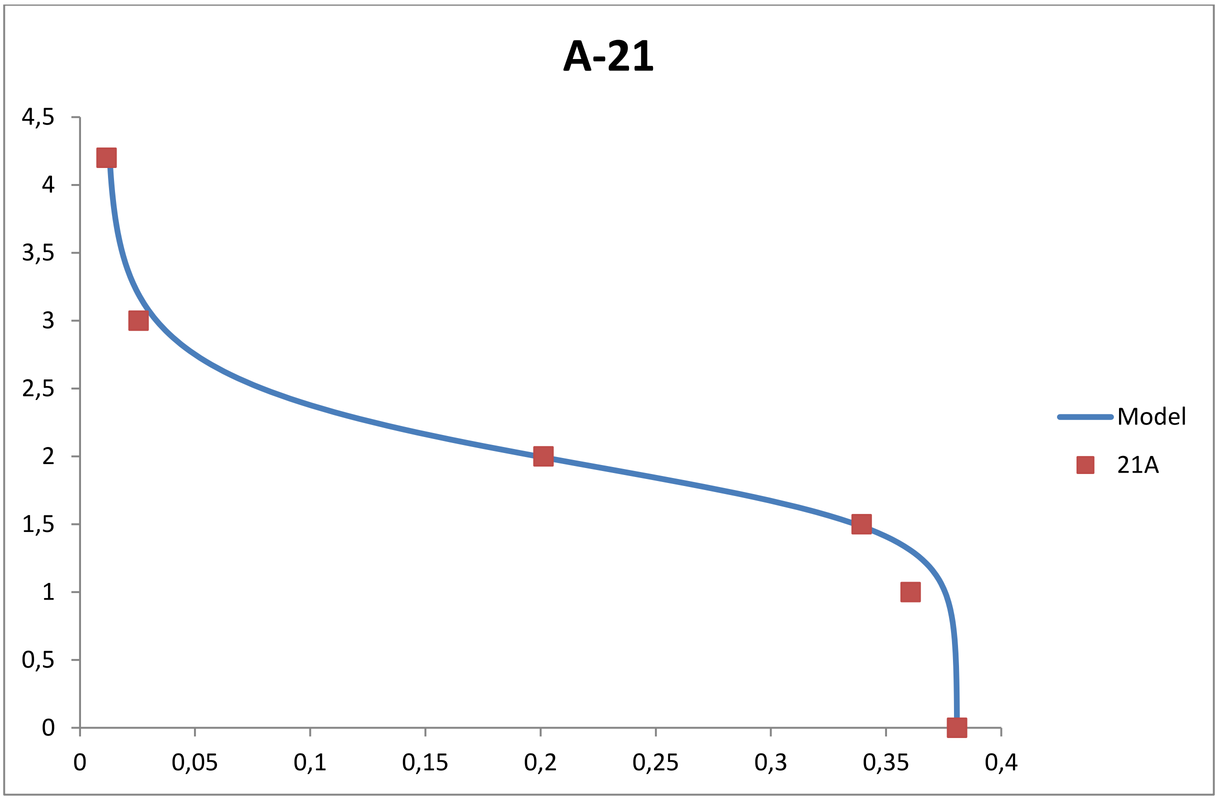

A-21
4,5
4
3,5
3
2,5
2
1,5
1
0,5
0
0
0,05
0,1
0,15
0,2
0,25
0,3
0,35
0,4
Model
21A